Sandra Cristina Vale Rodrigues

Preparation of Collagen-Hydroxyapatite Biocomposite Scaffolds by Cryogelation Method for Tissue Engineering Applications

Tese submetida à Faculdade de Engenharia da Universidade do Porto
para candidatura à obtenção do grau de Mestre em Engenharia Biomédica

Faculdade de Engenharia

Universidade do Porto

Julho 2011

This thesis was supervised by:

Professor Fernando Jorge Monteiro (supervisor)
Faculdade de Engenharia, Universidade do Porto
INEB – Instituto de Engenharia Biomédica, Laboratório de Biomateriais, Universidade do Porto

Doutora Christiane Laranjo Salgado (co-supervisor)
Faculdade de Engenharia, Universidade do Porto
INEB – Instituto de Engenharia Biomédica, Laboratório de Biomateriais, Universidade do Porto

The research described in this thesis was conducted at:

INEB – Instituto de Engenharia Biomédica, Laboratório de Biomateriais, Universidade do Porto

…to Bruno and my Parents

“Those who dream by day are cognizant of many things

which escape those who dream only by night”

Edgar Allan Poe

Acknowledgments

I would like to show my deepest appreciation to the persons who helped me during this project and made this thesis possible.

Firstly, I would like to express my gratitude and esteem to my supervisor, Professor Fernando Jorge Monteiro, for his unending enthusiasm and patience, his permanent support, help and friendship during the development of this work.

I also would like to thank my co-supervisor, Dr. Christiane Laranjo Salgado, for her advice, support, help and encouragement.

My thanks to Dr. Abhishek Sahu for his sympathy, help and availability during this journey.

My special thanks to Professor Maria Helena Fernandes for getting me started with cell culture experiments, her constant help and availability. I also like to thank to Mónica Garcia from Faculdade de Medicina Dentária da Universidade do Porto, for her kind assistance in cell work.

I would like to acknowledge the friendship of everyone at INEB during my work.

I am also very grateful to Ricardo Vidal from INEB for the assistance in FTIR and to Daniela Silva and Rui Rocha from CEMUP for the assistance in SEM analysis.

Finally, I would like to deeply express my gratitude to my parents and my sister for their patience, encouragement and continuous support. A special thanks to Bruno for his constant comprehension, support and unconditional help.

Abstract

The available treatments for repairing injured bone tissues could induce many problems and are often unsatisfactory. Bone tissue engineering is a very promising approach for the treatment of damaged bone and to overcome current clinical limitations. Recent efforts of bone repair focus on development of porous three dimensional scaffolds for cell adhesion and proliferation. In this work, collagen-nanoHA cryogel scaffolds (70:30; 50:50; 30:70 mass percentage) were produced by cryogelation technique using EDC and NHS as crosslinking agents. A pure collagen scaffold was used as control. Morphology analysis (SEM) revealed that all cryogel scaffolds had highly porous structure with interconnective porosity and the nanoHA aggregates were also randomly dispersed throughout the scaffold structure. Chemical analysis (FTIR) showed the presence of all major peaks related to collagen and hydroxyapatite in the biocomposite scaffolds and also indicated possible interaction between nanoHA aggregates and collagen molecules. Porosity analysis revealed an enhancement in the surface area as the nanoHA percentage increased in the collagen structure. The biocomposites showed improved mechanical properties (E') as the nanoHA content increased in the scaffold. As expected, the swelling capacity decreased with the increase of nanoHA content. The scaffolds degradation, mediated by collagenase, increased as the nanoHA percentage increase in the polymer matrix. However, differences between collagen and collagen-nanoHA biocomposite scaffolds were not statistically significant. *In vitro* biological studies using human osteoblast-like cells (MG63) showed that the cells had a normal morphology and they were able to attach and spread out in all cryogels surfaces. The results suggest that the presence of collagen-nanoHA biocomposite scaffolds resulted in higher overall cellular proliferation compared to pure collagen scaffold. A statistically significant difference between collagen and collagen-nanoHA cryogels was observed after 21 day of cell culture. Histological analysis of the cell-seeded scaffolds using hematoxylin-eosin staining revealed also that collagen scaffold presented lower cell density than biocomposite scaffolds. The results of the present study suggest that the

collagen-nanoHA cryogels could have potentially appealing application as scaffolds for bone regeneration.

Key-words: Biomaterials, Bone Tissue Engineering, Cryogels, Nanohydroxyapatite, Collagen.

Resumée

Les traitements disponibles pour la réparation du tissu osseux lésé peuvent induire beaucoup de problèmes et peuvent être souvent insuffisants. L'ingénierie du tissu osseux est un abordage qui promet en ce qui concerne le traitement des lésions osseuses et prétend dépasser les actuelles limitations cliniques. Les efforts récents vis-à-vis de la réparation osseuse se concentrent envers le développement des structures tridimensionnelles pour la concentration et prolifération cellulaire. Dans ce travail, des matrices de collagène et d' hydroxyapatite nanométrique (70:30; 50:50; 30:70 pourcentage en masse) ont été produites par la méthode de cryogélation, utilisant les agents de réticulation EDC et NHS. Une matrice de collagène a été utilisée comme contrôle. L'analyse de morphologie (SEM) a montré que toutes les matrices avaient une structure très poreuse, avec une porosité interconnectée et que les agrégés de nanohydroxyapatite étaient aussi aléatoirement dispersés par la structure de la matrice. L'analyse chimique (FTIR) a démontré la présence de toutes les radicaux chimiques, les plus importants liés au collagène et à l'hydroxyapatite dans les matrices biocomposites et a indiqué aussi une possible interaction entre les agrégés de nanohydroxyapatite et les molécules de collagène. L'analyse de la porosité a démontré une augmentation de la surface, due à l'augmentation du pourcentage de nanohydroxyapatite dans la structure du collagène. Les biocomposites ont montré des propriétés mécaniques meilleures (E') au fur et à mesure que la quantité de nanohydroxyapatite augmentait dans l'éponge. Comme on l´espérait, la capacité de dilatation a diminué, cela due a l'augmentation de la quantité de nanohydroxyapatite. La dégradation de la matrice, induite par la collagenase, a augmenté avec l'augmentation du pourcentage de nanohydroxyapatite dans la matrice polymérique. Cependant, les différences vérifiées entre les éponges de collagène et celles de collagène-nanohydroxyapatite n'ont pas été statistiquement expressives. Des études *in vitro* avec des cellules osseuses de l'ostéosarcome humain (MG63) ont montré que les cellules avaient une morphologie normale et ont été capables d'adhérer et de s'épanouir sur la surface de tous les cryogels. Les résultats ont permit d'établir que la présence

des matrices biocomposites a conduit à une plus grande prolifération cellulaire en comparaison avec la matrice de collagène pur. On a observé une grande différence statistique entre les matrices de collagène et de collagène-nanohydroxyapatite après 21 jours de culture cellulaire. L'analyse histologique des matrices parsemées de cellules, utilisant une coloration de hématoxyline-éosine, a démontré elle aussi que la matrice de collagène présentait une densité cellulaire plus petite que la matrice de biocomposite. Les résultats de l'étude effectué suggèrent que les cryogels de collagène-nanohydroxyapatite pourront avoir une application vraiment intéressante comme des matrices pour la régénération osseuse.

Mots-clés : Biomatériaux, L'ingénierie du tissu osseux, Cryogels, Nanohydroxyapatite, Collagène.

Resumo

Os tratamentos disponíveis para reparação do tecido ósseo lesado podem induzir muitos problemas e podem ser frequentemente insatisfatórios. A engenharia do tecido ósseo é uma abordagem muito promissora para o tratamento de lesões ósseas e para ultrapassar as actuais limitações clínicas. Recentes estudos na reparação óssea focam-se no desenvolvimento de estruturas tridimensionais para adesão e proliferação celular. Neste trabalho, matrizes de colagénio e hidroxiapatite nanométrica (70:30; 50:50; 30:70 percentagem em massa) foram produzidas pelo método de criogelificação usando como agentes de reticulação EDC e NHS. Uma matriz de colagénio puro foi utilizada como controlo. A análise da morfologia (SEM) revelou que todas as matrizes tinham uma estrutura altamente porosa com poros interconectados e que as partículas de nanohidroxiapatite estavam também aleatoriamente dispersas pela estrutura da matriz. A análise química (FTIR) mostrou a presença de todos os picos importantes relacionados com o colagénio e com a hidroxiapatite nas matrizes de biocompósitos e também indicou uma possível interacção entre as partículas de nanohidroxiapatite e as moléculas de colagénio. A análise da porosidade revelou um aumento na área de superfície com o aumento da percentagem de nanohidroxiapatite na estrutura de colagénio. Os biocompósitos mostraram melhores propriedades mecânicas (E') à medida que a concentração de nanohidroxiapatite aumentava na esponja. Como esperado, a capacidade de absorção de líquidos diminuiu com o aumento da quantidade de nanohidroxiapatite. A degradação enzimática das matrizes, mediada pela colagenase, aumentou com o aumento da percentagem de nanohidroxiapatite na matriz polimérica. No entanto, as diferenças verificadas entre as esponjas de colagénio e as de colagénio e nanohidroxiapatite não foram estatisticamente significativas. Estudos *in vitro* com pré-osteoblastos de osteossarcoma humano (MG63) mostraram que as células possuíam uma morfologia normal e que foram capazes de aderir e espraiar-se na superfície de todos os criogéis. Os resultados sugeriram que a presença das matrizes de biocompósitos resulta, em geral, numa maior proliferação celular quando comparada com a matriz de colagénio puro. Uma

diferença estatística significativa na proliferação celular entre as matrizes de colagénio e as de colagénio-nanohidroxiapatite foi observada após 21 dias de cultura celular. Para a análise histológica das matrizes cultivadas com células foi utilizada a coloração de hematoxilina-eosina. Os resultados revelaram também que a matriz de colagénio apresentava menor densidade celular do que as matrizes de biocompósitos. Os resultados do presente estudo sugerem que os criogéis de colagénio-nanohidroxiapatite poderão ter um potencial para aplicação como matrizes para regeneração óssea.

Palavras-Chave : Biomateriais, Engenharia do tecido ósseo, Criogéis, Nanohidroxiapatite, Colagénio.

Contents

List of Figures

List of Tables

List of abbreviations

3D	Three-dimensional
ALP	Alkaline phosphatase
CLSM	Confocal laser scanning microscopy
CO_2	Carbon dioxide
DAPI	4’,6-diamino-2 phenylindole
DMA	Dynamic mechanical analysis
DNA	Deoxyribonucleic acid
ECM	Extracellular matrix
EDC	1-ethyl-3-(3-dimethyl aminopropyl) carbodiimide hydrochloride
FBS	Fetal bovine serum
FTIR	Fourrier transform infrared spectroscopy
HA	Hydroxyapatite
HCl	Hydrochloric acid
H&E	Hematoxylin and eosin
MSCS	Mesenchymal stem cells
NanoHA	NanoHydroxyapatite
NHS	N- Hydroxysuccinimide
PBS	Phosphate-buffered saline
SEM	Scanning electron microscopy
ULMP	Unfrozen liquid microphase
α-MEM	Alpha minimum essential medium

Chapter I

Introduction

Introduction

1. Bone

Bone is a living, highly vascularized, dynamic, mineralized connective tissue that forms the skeleton of most vertebrates [1, 2]. Bone is characterized by its hardness, resilience and growth mechanisms, and its ability to remodel and repair itself [1]. It has been well studied by the materials engineering community because of its unique structure and mechanical properties [3]. In simple terms, bone is a dense multi-phase material or “composite” made up of cells embedded in a matrix composed of both organic and inorganic elements [1]. However, its structure and proportion of its components differ widely with age and site, resulting in many different classifications of bone that exhibit very different mechanical and functional characteristics [1].

Scale is very important in describing hierarchical architecture of bone and understanding relationship between structures at various levels of hierarchy. There are three levels of structures: (1) the nanostructure (a few nanometers to a few hundred nanometers), such as non-collagenous organic proteins, fibrillar collagen and embedded mineral crystal; (2) the microstructure (from 1 to 500 μm), such as lamella, osteons and Haversian systems; (3) the macrostructure, such as cancellous and cortical bone [4]. These three levels of oriented structures assemble into the heterogeneous and anisotropic bone, as shown Figure 1.

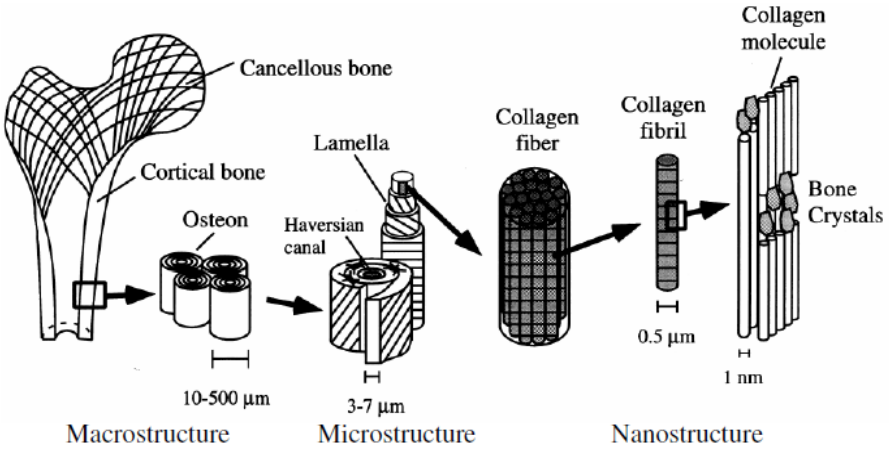

Figure 1. Hierarchical architecture of bone [4].

1.1. Bone function

The complex organization and incomparable properties of bone tissue allow it to perform a variety of unique functions in the body. The skeleton is designed to protect vital organs of the body and provide the frame for locomotion of the musculoskeletal system. Tissue properties of bone as well as the structure of whole bones contribute to the exceptional stiffness and strength. These exceptional properties give bone the ability to withstand the physiological requests without breaking [5]. Furthermore, bone is a reservoir for many essential minerals, such as calcium and phosphate, and plays an important role in the regulation of ion concentrations in extracellular fluid [5]. Bone marrow contains mesenchymal stem cells (MSCs), which are multipotent cells capable of differentiation into bone, cartilage, tendon, muscle, skin, and fat tissue [5]. In this cavity, there are also different kinds of hematopoietic cells that produce the red and white blood cells. These cells have the function of gas transportation (oxygen and carbon dioxide) and immune resistance, respectively [5].

1.2. Bone Structure

The adult human skeleton is composed of 80% cortical bone and 20% trabecular bone (Figure 2). Different bones in the body show different percentages of cortical and trabecular bone [6].

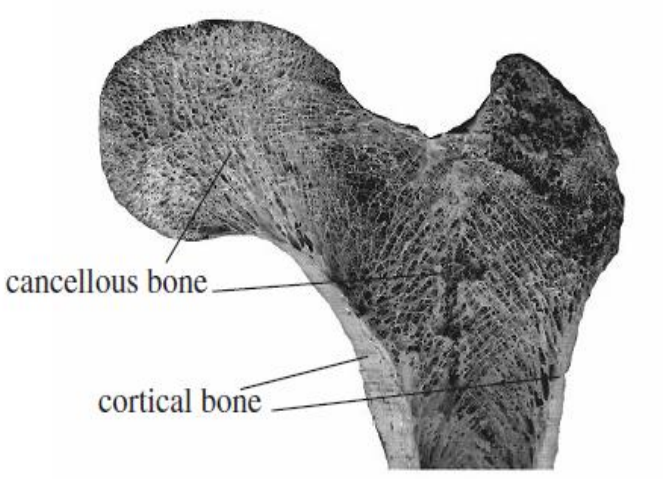

Figure 2. Cancellous Bone vs. Cortical Bone [1].

Cortical bone is hard and dense and makes up the shaft surrounding the marrow cavity of long bones [5, 7]. Cortical bone has only 10% of porosity, allowing space for only a small number of cells and blood vessels. The structural unit of cortical bone is the cylindrically shaped osteon, which is composed of concentric layers of bone called lamella [5, 7]. Blood vessels are present along the Haversian canals located at the center of each osteon. The nutrient diffusion is further allowed by canaliculi, or microscale canals within the bone [5]. Osteons are aligned in the longitudinal direction of bone and therefore, cortical bone is anisotropic [5].

Cancellous bone, a porous trabecular bone, is found in the ribs, spine, and the ends of long bones [5, 7]. Trabecular bone, which may has as much as 50–90% pores, is an interconnected network of small bone trusses (trabecula) aligned in the direction of loading stress. The porous of cancellous bone contains vessels and bone marrow, which provide lower mechanical support compared to cortical bone [5].

1.3. Bones Surfaces

Cortical bone has an outer and an internal surface which contains the bone marrow cavity (Figure 3). The outer surface is covered by the periosteum, a fibrous connective tissue sheath which contains blood vessels, nerve fibers, osteoblasts and osteoclasts cells [8]. The periosteum is tightly attached to the outer cortical surface of bone by thick collagenous fibers, called Sharpeys' fibers, which extend into underlying bone tissue. Periosteal surface activity is important for appositional growth and fracture repair. Bone formation typically exceeds bone resorption on the periosteal surface, so bones normally increase in diameter with aging [8].

The internal surface is covered by the endosteum, a membranous structure also covering the trabecular bone surface, and the blood vessel canals (Volkman's canals) present in bone. The endosteum is in contact with the bone

marrow cavity, trabecular bone, and blood vessel canals and contains blood vessels, osteoblasts, and osteoclasts cells [8].

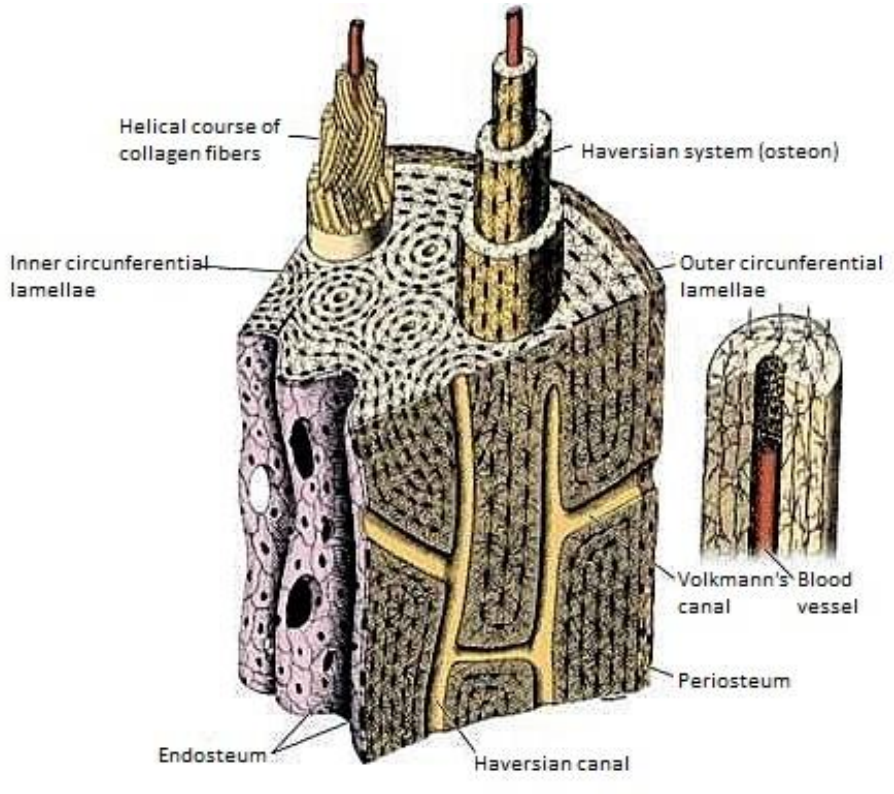

Figure 3. Outer and internal surface of bone [9].

1.4. Bone cells

Three types of differentiated cells inhabit the organic-inorganic composite structure of bone. These cells are osteoblasts, osteoclasts and osteocytes [4, 5, 8]. All of them have defined responsibilities and as a result are fundamental for the maintenance of a healthy bone tissue.

Osteoblasts

Osteoblasts, derived from MSCs, are located on the bone surfaces, side by side, and are responsible for secrete collagenous proteins that form the organic matrix of bone. This matrix becomes then calcified, but just how this mineralization is brought about remains controversial [4, 5, 10]. Osteoblasts

also manufacture hormones, such as prostaglandins, to act on bone itself. They robustly produce alkaline phosphatase, an enzyme that has a role in bone mineralization. Once surrounded by calcified matrix, the osteoblasts are called osteocytes (Figure 4).

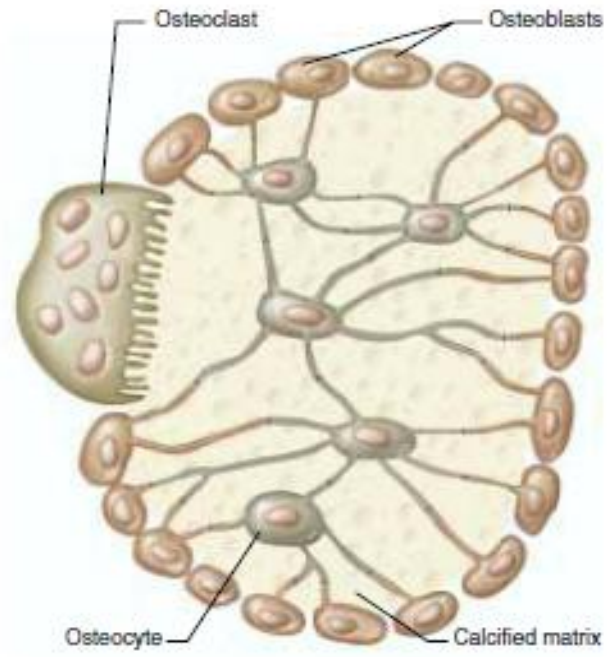

Figure 4. Cross-section of a small bone portion. The osteocytes have long processes that extend through small canals and connect with each other and to osteoblasts with tight junctions [11].

Osteocytes

Osteocytes play an important role in detecting and then converting mechanical stimuli into biochemical molecules that should stimulate bone production or resorption [5]. Bone tissue is exposed to a variety of mechanical stimuli, including shear forces associated with fluid flow; therefore, cellular signals and response are essential for proper maintenance of bone [5].

Osteoclasts

The third cell type, osteoclast, is responsible for bone resorption [5, 8]. Osteoclasts are large, terminally differentiated, multinucleated cells that have well defined and developed organelles. These cells are usually located within the tissue layer lining the endosteal surface or the connective tissue layer lining the periosteal surface [12]. These differentiated cells are fundamentally characterized by their primary and exclusive function – to degrade bone tissue – regardless of their localization or properties. Unlike osteoblastic cells, osteoclasts are derived from hematopoietic cell lines of macrophage/monocyte linage [12]. Osteoclasts differentiation occurs within the bone microenvironment, where interaction between monocyte precursors and osteoblasts enables the cells to differentiate into osteoclasts [12].

1.5. Extracellular Matrix

As above mentioned, bone is involved in a series of processes, which are found to be essential for the human body. Most of the outstanding properties of bone are related to its matrix constitution. The ECM play many roles, such as providing support and anchorage for cells, segregating tissues from one another and regulating intercellular communication [13]. In concert with cell-intrinsic regulatory cascades, these temporally and spatially coordinated signals instruct cells to acquire specific fates, controlling for example cell development, proliferation, migration and function [14, 15]. On the other hand, cells are constantly secreting signals that can trigger structural and biochemical microenvironment changes, as it is most evident during proteolytic remodeling of the ECM [14]. Therefore, cell-matrix interactions play crucial roles in tissue development and remodeling [16].

The extracellular matrix has two main components: a mineral part, which contributes with 65-70% to the matrix and, an organic part that comprises the remaining 25-30% of the total matrix [6]. Because of this, and from a materials science perspective, bone can be considered as a truly composite material [6].

1.5.1. Organic Phase

Several different proteins with different applications constitute the organic phase of bone matrix [6]. Mainly it is constituted by type I collagen, glycosaminoglycans, proteoglycans and glycoproteins [17]. However, approximately 90% of the organic phase of bone is Type I collagen [4].

The linear molecules (or fibers) of Type I collagen are self-assembled in triple helix bundles having a periodicity of 67 nm, with 40 nm gaps (called hole-zones) between the ends of the molecules and pores between the sides of parallel molecules [4]. Collagen fibers provide the framework and architecture of bone while hydroxyapatite (HA) crystals are located within or between fibers [4]. Figure 5 shows the molecular arrangement of collagen and hydroxyapatite crystals in bone.

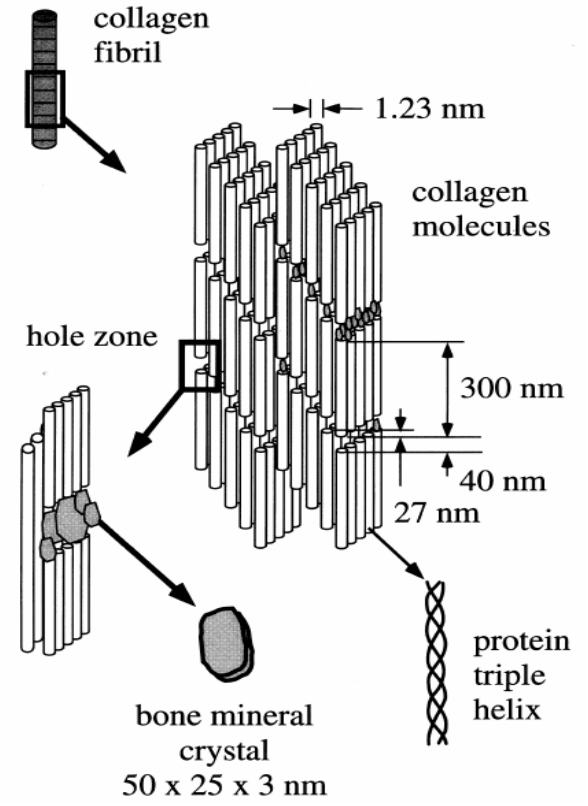

Figure 5. A schematic diagram illustrating the assembly of collagen fibers and bone minerals crystals [4].

Collagen

Collagen is the primary structural material of vertebrates and is the most abundant mammalian protein accounting for about 20–30% of total body proteins [18]. It is present in a number of different connective tissues both calcified and non-calcified for primarily mechanical function [1,18]. Collagen plays an important role in the formation of tissues and organs, and it is involved in various functional expressions of cells [18]. At least 22 types of collagen have been reported [18]. The main types of collagen found in connective tissues are types I, II, III, V and XI. However type I is the main collagen of skin and bone and therefore is the most abundant form, accounting for 90% of the body's total collagen [1,14]. The collagen molecule consists of carefully arranged arrays of tropocollagen molecules, which are long rigid molecules composed of three left-handed helices of peptides and these associate laterally to form collagen fibrils with a characteristic banded structure [1]. Finally, fibrils associate to form the collagen fibers (Figure 6).

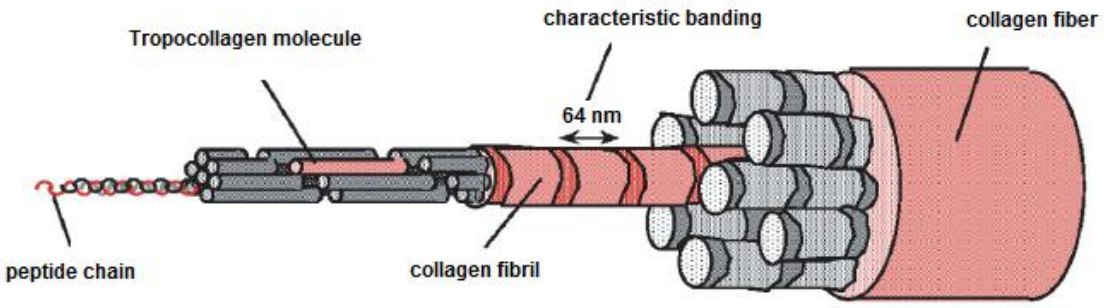

Figure 6. Hierarchical organization of collagen fibers [1].

Collagen has increasingly been used as a biomaterial during the last few decades, which has been reflected both in the number of published research articles and the introduction of new collagen-based systems onto the market [19-30]. Many natural polymers and their synthetic analogues are used as biomaterials, but the characteristics of collagen as a biomaterial are distinct

from those of synthetic polymers mainly in its kind of interaction to the body [18].

Collagen properties include excellent biocompatibility, biodegradability, easy absorption in the body and weak antigenicity, which made collagen a primary resource in medical applications [18]. Moreover, it can be prepared in a number of different forms including sheets, sponges and beads and can be solubilized into an aqueous solution, particularly in acidic aqueous media. Collagen is relatively stable due to its function as the primary structural protein in the body, although, it is still liable to enzymatic degradation by collagenase enzyme [18].

1.5.2. Inorganic Phase

The inorganic phase (or mineral phase) consists mainly of bone apatite, a crystal of a calcium phosphate type. Calcium phosphate is a mineral which consists of both calcium ions (Ca^{2+}) and orthophosphates (PO_4^{3-}), metaphosphates or pyrophosphates ($P_2O_7^{4-}$) and occasionally hydrogen or hydroxide ions [31]. Despite carbonate, citrate, magnesium, fluoride, hydroxyl, potassium and other ions can be found in smaller amounts, the major mineral phase of bone is hydroxyapatite. This bioactive hydrated calcium phosphate has a Ca:P ratio of 1,67, an hexagonal structure with a chemical formula $Ca_{10}(PO_4)_6(OH)_2$ (Figure 7) [32].

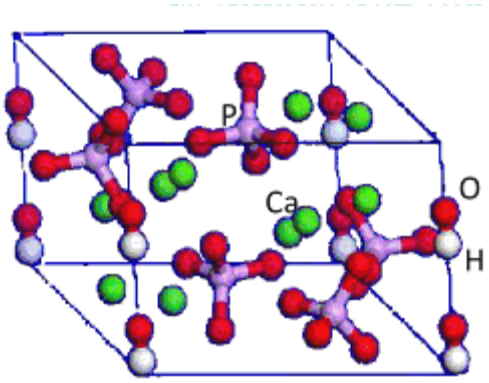

Figure 7. Crystal structure of hydroxyapatite [33].

Nanostructured hydroxyapatite

Hydroxyapatite remains the most promising ceramic of all calcium phosphate materials for bone tissue engineering [34]. It has a similar chemical composition and structure to the mineral component of natural bone and has showed high biocompatibility, osteoconductivity and bone bonding ability [35, 36]. It develops a direct, adherent and strong bonding with bone tissue. This material subsequently recruits bone cells (osteoblasts) which proliferate and produce bone matrix [37]. Moreover, unlike the other calcium phosphates, hydroxyapatite does not solubilize under physiological conditions, being thermodynamically stable at physiological pH [38]. Recent studies have suggested that better osteoconductivity would be achieved if synthetic hydroxyapatite could resemble bone minerals more in terms of composition, size and morphology. Moreover, it has been recognized that nanohydroxyapatite may have other special properties due to its small size and huge specific surface area. Due to its properties, hydroxyapatite has been widely used to fill, extend and repair damaged bone tissue. It can also be used in soft tissue. This biomaterial can be obtained from mammal bones or coral [39].

For the synthetic hydroxyapatite preparation several techniques have been employed, including hydrothermal reaction, sol-gel synthesis, pyrolisis of aerosols and micro-emulsion, biomimetic process and chemical precipitation [39]. Chemical precipitation is the most used alternative for the preparation of fine HA powders and it was employed by Fluidinova S.A. to produce the nanoHA particles used in this work.

1.6. Bone remodeling, healing and repair

After a fracture has occurred, a number of events proceed to initiate the healing and repairing process [39]. First, growth and differentiating factors are activated by the injury process, which in turn activates multipotent osteoprogenitor cells [39]. These cells produce a class of proteins known as

bone morphogenetic proteins (BMPs), which are intimately bound to collagen. These osteoconductive proteins, along with other growth factors, cytokines, and hormones, induce the migration of adult mesenchymal cells and their differentiation into bone-forming cells [39].

As in other tissues, bone repair is a continuous process that sets a cascade of events into motion. These events are shown in Figure 8.

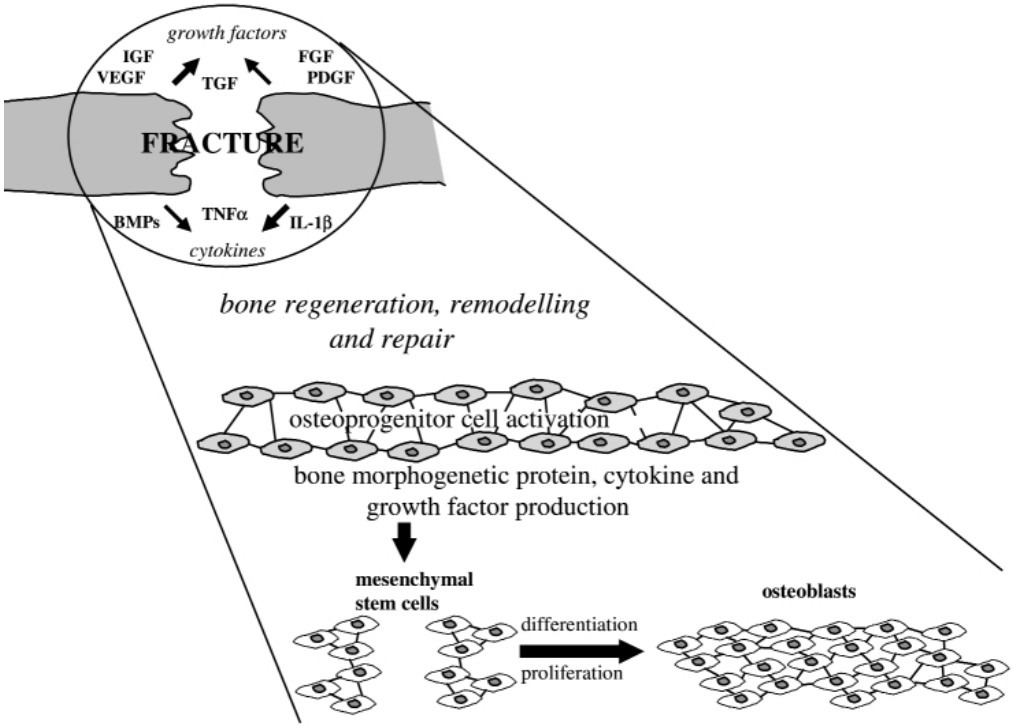

Figure 8. Cytokines cascade and cellular events during the bone regeneration, remodeling, and repair process [39].

1.7. Current and modern treatments for bone defects

Among bone repair methods, autograft transplants are considered to be the main clinical method (gold standard) [4, 40]. Autograft implant is the tissue removed from one portion of the skeleton and transferred to another location of the same individual. It is commonly collected in the form of cancellous bone from the patient's iliac crest, but compact bone can be used as well [4, 6]. Autograft transplants bring osteogenic, osteoinductive and osteoconductive

components to the defect sites without triggering host immune response. However, as the quantity of bone tissue that can be obtained for autograft implant is limited, and because it requires an extensive operation which may cause morbidity, pain and possible infection of the donor site, there are many ongoing attempts to search for alternatives [40-42].

Allograft bone transplantation is a potential alternative which overcomes the problem of quantity as it can be obtain from cadaver tissue. Allograft disadvantages, however, include less osteoinductivity [40], possible trigger of host immune response and likely transmission of some diseases [4, 40].

Due to the above stated issues with autografts and allografts implants, metals and some ceramics have been the materials used as materials of choice for numerous orthopedic applications for a long implantation time [6, 40]. Although metals are still the most used alternative for severe bone fractures, they do not exhibit the physiological, dynamic and mechanical characteristics of true bone and therefore they cannot perform as well as healthy bone [4]. Mismatches in the mechanical properties of metal implants and physiological bone result in “stress shielding” problems. That is, the implanted material shields the healing bone from mechanical request, resulting in localized bone resorption, necrosis of the surrounding bone and subsequent implant failuring [4]. This condition should create some clinical complications and could require additional surgery to remove the implants and the surrounding necrotic bone tissue. In addition to the “stress shielding” problems, insufficient osseointegration or lack of strong bone/material interface binding may also lead to implants failure or fibrous tissue ingrowth [4]. Both outcomes may consequently lead to clinical failure and further revision surgery [4]. On the other hand ceramics have very low tensile strength and are brittle, thus they cannot be used in locations where significant torsion, bending, or shear stresses are present [6].

Synthetic materials or alloplasts are being suggested as a choice for application in bone regeneration, but these first generation materials are not particularly appropriate as the host treats them as foreign bodies and creates a

thin fibrous membrane around them [40]. This prevents the alloplast from being integrated into the host tissue and consequently becoming isolated [40].

Hence it is clear that an adequate bone replacement is so far to be found and it is at the same time urgently needed to achieve full recovery of many orthopedic patients. A possible solution for these problems may reside in Tissue Engineering [6].

Nowadays, bone constructs are elaborated according to tissue engineering principles and they are looked upon as an ideal choice to reconstruct bone segmental defects. The objective of this strategy is indeed to overcome the limitations exhibited by transplantation of tissue grafts and biomaterials. Therefore, bone tissue engineering offers a promising new approach for bone repair [40].

2. Tissue Engineering. General Aspects

Tissue engineering is a recent field that is rapidly growing in both scope and importance within biomedical engineering. It represents the connection between the rapid developments in cell and molecular biology, materials science, chemical, and mechanical engineering [43]. The ability to manipulate and reconstruct the tissue function has tremendous clinical implications and could play a major role in cell and gene therapies during the next few years in addition to expand the tissue supply for transplantation therapies [43].

The term *tissue engineering* was initially defined by the attendees of the first NSF sponsored meeting in 1988 as “application of the principles and methods of engineering and life sciences toward fundamental understanding of structure function relationship in normal and pathological mammalian tissues and the development of biological substitutes for the repair or regeneration of tissue or organ function [44].” In 1993, Langer and Vacanti summarized the early developments in this field and defined tissue engineering as “an interdisciplinary field that applies the principles of engineering and life sciences toward the development of biological substitutes that restore, maintain or improve tissue or organ function” [44].

The goal of tissue engineering is to overpass the limitations of conventional treatments based on organ transplantation and biomaterial implantation [45]. Through this technology, tissue loss or organ failure may be treated either by implantation of an engineered biological substitute or alternatively with *ex vivo* perfusion systems. Tissue engineering has therefore attracted great attention in science, engineering, medicine and in the society. The tissue engineering products may be fully functional at the time of treatment (e.g., liver assisting devices, encapsulated islets), or may have potential to integrate and form the expected functional tissue upon implantation (e.g., chondrocytes encapsulated in a matrix carrier) [44]. The reconstruction of a new tissue by tissue engineering should need some components. These include: (1) cells; (2) biomaterials as scaffolds substrates; and (3) growth factors that promote and/or prevent cell migration, adhesion, proliferation, and differentiation by up-regulating or down-regulating the synthesis of proteins and growth factors (Figure 9) [46].

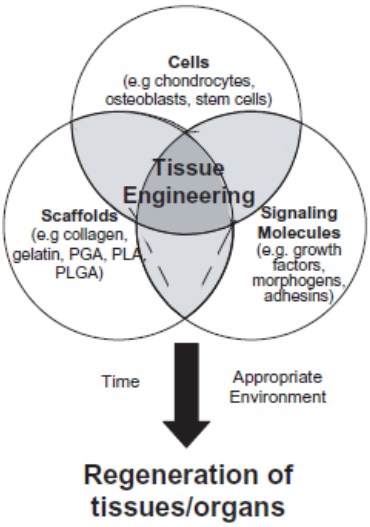

Figure 9. Tissue Engineering Triad [46].

The basic principle of Tissue Engineering is illustrated in Figure 10. Cells are collected from the donor tissue and expanded in laboratory. Once there are enough cells, they can be seeded with signaling molecules on a scaffold substrate and cultured *in vitro*. When the construct is matured enough, it can be implanted at the desired site [47, 48]. Therefore, highly porous scaffolds have a

critical role in cell seeding, proliferation and new tissue formation in three dimensions [49]. Scaffolds are 3D substrates for cells and their main goal is to be a template for tissue regeneration [50]. The ideal scaffold must be biocompatible, non-immunogenic, have an interconnected porous network to allow cell penetration and transfer of nutrients, oxygen and waste products, sufficient surface area and a diversity of end terminals (i.e CH_3-; OH-) that promote cell migration, adhesion, differentiation and proliferation. Also the scaffold must possess a degradation rate that closely matches the regeneration rate of the new tissue [51, 52].

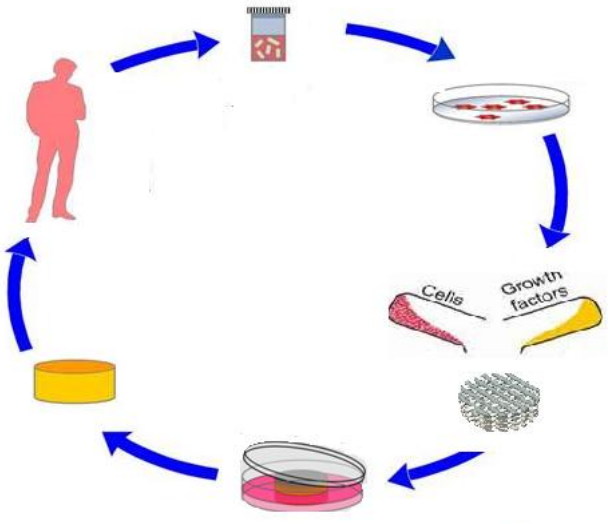

Figure 10. Basic Principle of Tissue Engineering.

2.1. Bone Tissue Engineering: Promises and Challenges

As previously mentioned, compared to traditional procedures, bone tissue engineering techniques based on autogenous cell/tissue transplantation would eliminate problems of donor compatibility, supply limitation, pathogen transfer and immune response. Consequently, it has become a rapidly expanding research area since it immerges from the concept of tissue engineering [49].

Bone Engineering typically uses an artificial extracellular matrix (or scaffold), osteoblasts or cells that can become osteoblasts (i.e. bone marrow mesenchymal stem cells) and regulating factors that promote cell adhesion, differentiation, proliferation and bone formation [49]. Figure 11 shows the bone

tissue engineering concept using a hypothetical example of a femur. As it may be seen, a tissue substitute is constructed in the laboratory by combining a scaffold with living cells and growth factors. When the construct is mature enough, it is implanted on the patient to repair the bone femur.

Currently, the scientific challenges of bone tissue engineering are developing suitable 3D scaffolds that act as a template for cell adhesion and proliferation in favored 3D orientations. The scaffolds provide the necessary support for the cells to proliferate, and their architectures define the ultimate shapes of new bones [4]. Over the past decade, one of the main goals of bone tissue engineering has been to develop biodegradable materials as bone substitutes for filling large bone defects. In addition, such scaffolds must allow the proper diffusion of oxygen and nutrients for the seeded cells on the scaffold as well as proper diffusion of waste out of the materials. The final goal is to return full biological and mechanical functionality to a damaged bone tissue [4].

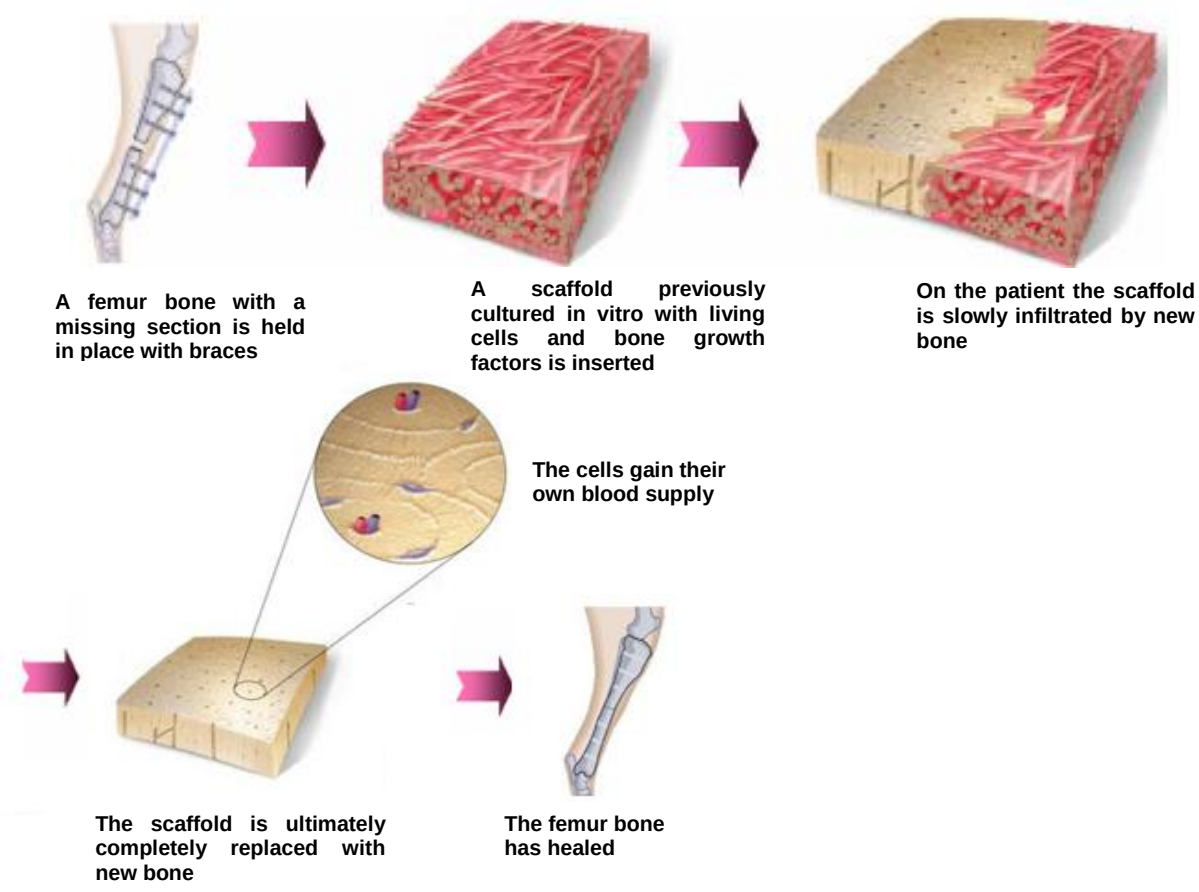

Figure 11. Schematic diagram of bone tissue engineering concept [4].

2.2. Essential requirements of scaffolds for bone tissue engineering

The requirements for a scaffold to be considered suitable for tissue engineering applications are complex and in many cases there is no full agreement among the biomaterials research community about the specific demands that are required for a particular tissue application. These requirements depend mainly on the tissue to be repaired and on the place and size of the damaged area [53, 54]. Nevertheless, there are some general key characteristics that a scaffold for bone tissue engineering must possess:

2.2.1. Biocompatibility

The ideal scaffold must be biocompatible. The materials and their degradation products should not involve an undesirable immune response or toxicity [55-58].

2.2.2. Appropriate mechanical properties

Appropriate mechanical properties are essential to offer the correct stress environment for the neo-tissue [55-59]; the mechanical strength of the scaffold should be enough to provide mechanical stability to withstand the stress before the synthesis of the ECM by the cells [50].

2.2.3. Controlled degradation rate

The scaffolds should be biodegradable and bioresorbable with a controllable degradation and resorption rate to match with the cell/tissue ingrowth as *in vitro* or *in vivo* evaluation [50]. The degradation rate of the scaffolds and the rate of new tissue formation must be coupled appropriately to each other in such a way that by the time the injury site is totally regenerated, the scaffold shall be totally degraded [50].

2.2.4. Appropriate pore size and morphology

Pore structure and pore size are important factors that are associated with nutrient supply to transplanted cells. Small diameter pores are preferable to yield high surface area per volume, as long as the pore size is greater than the diameter of a cell in suspension (typically 10 μm) [55, 57, 58]. Pores (less than 10 μm) are needed for cell-matrix interactions [60]. Although it is well established that pores diameters should be larger than 100 μm for bone ingrowth [61], there is a lack of consensus regarding the optimal pore size for maximum tissue ingrowth and/or for an optimal tissue engineering application. Some authors claim that a maximal tissue ingrowth is attained with a pore size ranging from 100 to 150 μm [57], but for others it should reach pores ranging from 100 to 350 μm [62], for instance.

Interconnectivity between pores is highly desirable since an interconnected pore network structure enhances the diffusion of the supplements on the scaffold and facilitates vascularization, thus it should improve the oxygen and nutrients supply to cells inside the scaffold and facilitated the waste transfer out of the scaffold [61].

2.2.5. Appropriate surface chemistry

The scaffolds should have appropriate surfaces to enhance cell adhesion, proliferation and differentiation. Most organ-cell types require the presence of a suitable substrate to retain their ability to proliferate and perform different functions since cell adhesion is the pre-requisite for further cellular events, such as spreading, interconnection, migration and biosynthetic activity [55, 57, 58]. Therefore, the characteristics of materials' surface, such as topography, chemistry, surface energy or wettabbility, play an essential role in cell adhesion to biomaterials [55, 57, 58].

3. Scaffolds Production Methods

As mentioned before, scaffolds have to be produced to make the cell distribution possible and to direct their growth into three-dimensional volume. Scaffolds structure is directly related to production methods. Several techniques have been developed to produce 3D porous scaffolds. These include solvent-casting and particulate-leaching, gas foaming, phase separation, electrospinning, salt leaching, melt molding, rapid prototyping and freeze-drying [44, 63-68]. However, most of these traditional production methods are complex, require specific equipments, uses high temperatures or involves hazardous organic solvents [47].

Cryogelation is a simple method that uses ice crystals as templates to produces a porous structure without the involvement of organic solvents or any additives during the scaffolds production. A more detailed description of this method is described below.

3.1. Cryogelation Method: Overview

Cryogelation is a simple method to obtain macroporous scaffolds which has not been fully used in biomaterial science. Processes of cryogelation occur by non-deep freezing, storage in the frozen state, and thawing of the solutions or colloidal dispersions containing monomeric or polymeric precursors potentially capable to produce gels. Polymeric materials formed under these conditions are called cryogels (cryos – frost, ice), and they have some specific features comparing to conventional gels [69-71]. The general method of cryogelation is showed in Figure 12.

When the initial solution is frozen not lower than ten degrees from the crystallization point of the pure solvent, the resulting solution looks as a single mass but is not completely solid: along with solvent-shaped crystals (ice in the case of aqueous systems), it includes some amount of the unfrozen liquid, where the gel main components are concentrated [69-71]. This cryoconcentrate is called the *unfrozen liquid microphase* (ULMP) [70]. After thawing the cryogel,

a system of large interconnected pores is formed within the material [72].Thus, polycrystals of the frozen solvent act as a porogen during cryogel formation [72]. Depending on the properties, the initial concentration of the precursors and conditions of the cryogenic processing, it could produce microporous scaffolds on the pore cross-section in the range of 0.1-10 μm or macroporous sponge-like cryogels possessing pore size up to 200 μm in cross-section [73-76].

The wide pores in the cryogels are interconnected, because during freezing of the initial solution, each crystal of the solvent grows until it begins to contact with other adjacent crystal, and a labyrinth-like system of interconnected channels is formed after the frozen sample is thawed [70, 71]. One of the main advantages of the cryogelation technology is that it can modulate a range a properties such as porosity, size and shape, biochemistry of the pore wall surfaces and the degradation rate [73].

A simple approach, without the involvement of organic solvents or any additives during the production, simultaneously with an efficient control over the pore size, makes the cryogelation a favorable method compared with others techniques, previously mentioned, that are currently used for the production of a porous scaffolds. Moreover, this method is a more cost-efficient process than, for example, simply freeze-drying [73].

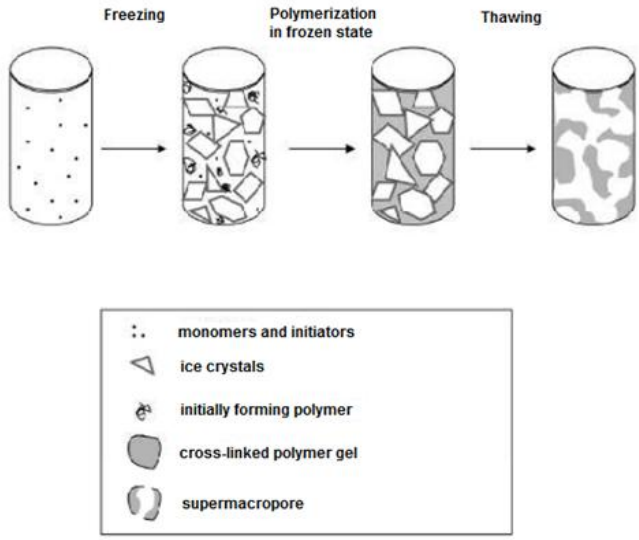

Figure 12. Scheme for the cryogelation method [76].

3.2. Cryogels as Potential Cells Scaffolds

Cryogels are gel matrices that are crosslinked at subzero temperatures using monomeric or polymeric precursors [71]. These gels can be obtained through the formation of both physically and covalently crosslinked homogeneous or heterogeneous polymer networks. As described before, at subzero temperature most of the solvent gels frozen while part of the solution is left unfrozen (so-called *unfrozen liquid microphase*) where the phases are separated (solvent and solute) after undergoing the chemical reactions [75]. These reactions in the liquid microphase lead to gel formation and the solvent crystals act as a porogen substrate. After thawing the ice crystals, a system of large interconnected pores is formed within the gel [71].

Cryogels Properties

Cryogels have some important general characteristics that include, interconnected highly porous structure, mechanical stability, elasticity, reversible and very rapid size change induced by to external forces and good swelling in aqueous media [72, 75]. Moreover, cryogels can be formed in any desirable shape, for examples, blocks, cylinders, tubes, granules and disks. Furthermore, they possess a spongy morphology that ensures unhindered convectional transport of solvents of practically any size, as well as mass transport of nano and even microparticles within the materials, although, in a traditional homophase gels, the diffusion of solvents could be a problem [71]. They are very tough, and can withstand high levels of deformations, might they be tensile, compressive or flexural strains [77]. However all these properties depend on the material used.

Cryogels Applications

Cryogels have been used in many applications of biotechnology and biomedicine, such as bio-separation technique, direct product recovery from fermentation media, separation of human blood lymphocytes and microbial cells as well as human tumor cells, chromatography support and also for immobilization of enzymes and cells (Figure 13) [71, 78].

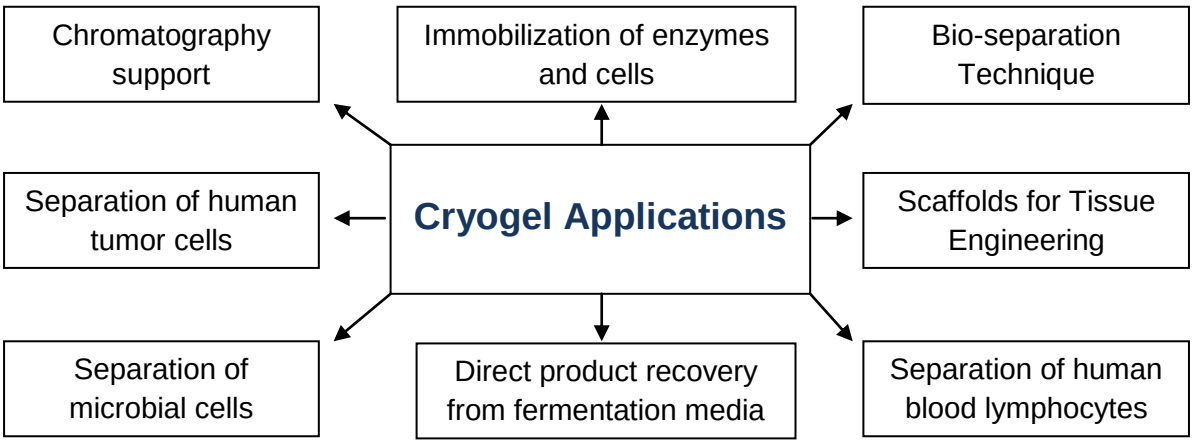

Figure 13. Scheme of Cryogel Applications.

But the application of cryogels as scaffolds for tissue engineering has not been extensively explored. Recently, few research groups have tried to explore this possibility. Bloch *et al* [79, 80] prepared agarose and agarose-gelatin scaffolds by cryogelation and studied the functional activity of pancreatic islets of male ICR mice, clonal insulinoma cells (INS-1E) and vascularization property for application in cell therapy of diabetes. Tripathi *et al* [81] have also prepared agarose-gelatin cryogel scaffolds and studied the attachment and growth of fibroblast cells. Similarly, a very recent study by Bhat *et al* [82] has showed that chitosan-agarose-gelatin cryogels are good 3D scaffolds for cartilage tissue engineering. Kathuria *et al* [72] were able to prepare porous cryogel scaffolds of high elasticity and mechanical strength by using chitosan and gelatin. Dainiak *et al* [73] showed that gelatin–fibrinogen cryogel dermal matrices are promising

material for wound repair. Singh *et al* [83] produced pHEMA-gelatin cryogels and have shown their potential application for skeletal muscle and cardiac tissue engineering.

4. *In Vitro* Cell Studies

In vitro cell culture is important as a preliminary model for screening the cell–material interaction without the complexity of the *in vivo* model [84, 85]. The cell culture experiments represent a simple and well-defined system [84]. The major advantage of using *in vitro* methods is the comparative cost effectiveness and speed of tests, which make them particularly suitable as a tool for screening large numbers of potential biomaterials and their modifications, allowing for a standardization/reproducibility of experimental conditions. This becomes even more relevant due to the background of current public (and expert) opinion that leads to a pressure for the reduction of animal experimentation whenever that is possible [86]. Coupled with this is the high sensitivity of the methods, which enables researchers to identify potentially cytotoxic materials at an early stage in the testing procedure [86]. These tests have been accepted as a very effective method for biocompatibility and toxicity testing [86]. However, *in vitro* methods have the problem of extrapolation to the *in vivo* situation and, in particular, to humans [86]. Therefore, *in vitro* testing represents always only one phase in studying biocompatibility [86]. The specimens classified as *in vitro* biocompatible must enter a further phase of testing, which requires *in vivo* observation and obtaining direct data from complex tissue systems [86].

4.1. Human Osteosarcoma Cell line (MG63)

For bone tissue engineering, primary osteoblast or cell lines are commonly employed [85]. The cell lines are used because they are representative of osteoblastic behavior since they display many characteristics of osteoblasts and they are easy to access since the stock is readily available [85]. Furthermore,

they are most resistant to stress conditions than primary cells. Primary cells on the other hand are not easily available and they do not always exhibit reproducible results due to variation in phenotypic expression from each isolation and loss of their phenotype with the time [85].

Despite being a tumor cell line, MG63 osteoblast-like cells exhibit many osteoblastic traits, which are characteristic of bone forming cells [87]. MG63 cells are originally isolated from human osteosarcoma and they have been well characterized and widely used for testing biomaterials [88]. The use of a secondary cell line, like this, provides a number of advantages, including absence of the individual variability present with the use of primary cell lines, better repeatability and reproducibility [87]. Therefore, the MG63 cell line represents a suitable *in vitro* model for studying the biocompatibility, the cell adhesion, spread and proliferation on biomaterials developed for tissue engineering applications [89].

4.2. Cell Culture Characterization

Cell culture characterization is usually based on the evaluation of several parameters characteristics of the cells in the culture, such as cell adhesion, growth, morphology and functional activity [90]. This characterization involves the use of several techniques that will be briefly described below.

4.2.1. Microscopy techniques

Scanning electron microscopy (SEM) and confocal laser scanning microscopy (CLSM) are qualitative methods commonly employed in order to evaluate some important characteristics of the cultured cells [91].

The high resolution of SEM makes it an ideal technique to study the sample's surface. Small structures may be identified on biological surfaces with high detail by using this technique [92].

CLSM is also a valuable tool for analyzing cells and tissue structures. Compared to conventional microscopic techniques it has the advantages of

increased image resolution and more sensitivity detection. Moreover, it offers the capability for 3D reconstruction, the elimination of out-of-focus images and optical sectioning of samples, eliminating artifacts seen in physically sectioned samples [93].

4.2.2. DNA extraction assay

Cell proliferation is the increase in cell number as a result of cell growth and division. One way to analyze cell proliferation is the measurement of DNA synthesis as a marker for proliferation [94]. The quantity of DNA per scaffold is assumed to be proportional to the number of cells per scaffold. Therefore, total DNA amounts can be quantified to assess cellular proliferation [94].

4.2.3. Alkaline phosphatase activity

The functional parameters of the cells in study can be evaluated by enzyme activity. In osteoblastic cultures, usually, it is evaluated the alkaline phosphatase (ALP) activity, which is one of the most commonly used biochemical markers for osteoblast activity [94]. Although ALP precise function is poorly understood, it is believed to play a critical role in skeletal mineralization. For that reason, ALP is routinely used in *in vitro* experiments as a marker of osteoblastic differentiation [95].

The aim of this work was to explore the possibility of applying cryogelation as an alternative technique to freeze-drying for preparation of 3D scaffolds based on collagen and collagen-nanohydroxyapatite composite that resembles bone matrix. Physical, chemical and morphological characterizations were performed with the produced scaffolds using different techniques. Finally, *in vitro* biological studies were evaluated using human osteoblast-like cells (MG63).

Chapter II

Materials and Methods

Materials and Methods

2.1. Materials

Type I collagen from bovine Achilles tendon was purchased from Sigma-Aldrich (St.Louis, USA). 1-ethyl-3-(3-dimethyl aminopropyl) carbodiimide hydrochloride (EDC) and N- Hydroxysuccinimide (NHS) were purchased from Fluka (Buchs, Switzerland). Hydrochloric acid (HCl) was obtained from Merck (Germany) and nano-hydroxyapatite aggregates (nanoHA) were kindly provided by Fluidinova (Maia, Portugal).

2.2. Preparation of collagen and collagen-hydroxyapatite cryogels

Type I insoluble collagen was swollen overnight in 5 mM HCl at 4°C at a concentration of 2 % (w/v). The dispersion was then homogenized (Ultra Turrax T25, IKA) at 11000 rpm and centrifuged at 2000 gf during 5 minutes.

The collagen cryogel was prepared with 5 ml of collagen slurry diluted in 4 ml of HCl (5mM) on ice bath. Subsequently, 10 mM NHS and 20 mM EDC were added to the collagen slurry and transferred to a syringe (Terumo Syringe, 5ml) that was used as a mold. This was then kept in a freezer at -18°C for 24 hours to complete the crosslinking. Afterwords, it was thawed at room temperature and the scaffold was washed with distilled water and finally dried with a freeze-dryer (Labconco, FreeZone 6) at - 80°C and 0.003 bar for 24 hours.

In the case of collagen-nanohydroxyapatite biocomposite scaffolds, the dry powders of nanoHA aggregates were mixed with the HCl solution in a particular ratio (final composition collagen-nanoHA 70:30, 50:50 and 30:70 w/w %) and then crosslinked as described above.

2.3. Characterization of Cryogels

2.3.1. Morphological Studies: Scanning electron microscope analysis

Morphology of cryogel samples was observed using scanning electron microscope (SEM, FEI Quanta 400FEG) operating at 15KV. Prior to SEM imaging, collagen and collagen-nanoHA scaffolds were cut with 0.4 cm length and 1 cm diameter and attached with Araldite^{TM} to aluminium sample holders. After, the samples were sputter-coated with palladium-gold (Bal–Tec–SCD 050). Image analysis through specific software (ImageJ, Wayne Rasband) was used to determine the scaffolds porous size range. The pore diameter for each sample was determined as:

$$D = [(4 \times A)/\Pi]^{1/2} \quad (1)$$

Where D and A were the pore diameter and the pore surface area, respectively. The total number of pores analyzed for each material was over 200.

2.3.2. FTIR

Dried samples (2 mg) were mixed with 200 mg of potassium bromide (KBr) and grounded into fine powders using an agate mortar and subsequently compressed into discs. Each disc was scanned at a resolution of 1 cm^{-1} over a frequency region of 400 to 4000 cm^{-1} using a FTIR spectrophotometer (Perkin Elmer, USA) and the characteristic peaks of IR transmission spectra were recorded. Each recorded spectrum was the average of 100 scans.

2.3.3. Mercury Intrusion Porosimetry

Mercury porosimetry method (Quantachrome Poremaster model No. 60) was used to evaluate total surface area, apparent density and porosity of collagen-nanoHA biocomposite cryogels. The referred equipment allowed the detection of open porous in the range [0.004-15.04] µm. Approximately 0.1 g of each scaffold was penetrated by mercury at high pressure and the reported data were obtained using Quantachrome Poremaster for Windows, version 3.0.

2.3.4. Swelling Properties Test

The swelling characteristics of materials are an important parameter to address how much and how quickly cryogels absorb the solvent from their surroundings. The swelling capacity studies were performed at room temperature by immersing weighed lyophilized samples with 9 mm diameter and 4 mm thickness in both aqueous phosphate-buffered saline (PBS) solution (Sigma) and distilled water. After all the time points, the samples were gently dried with a filter paper, this method was used to remove the solvent excess. The samples were weighed until 1 hour of immersion. At least three samples with similar weight (10 mg) were used for each kind of cryogel. The swelling equilibrium (Cw) was calculated as:

$$Cw\ (g.g^{-1}) = \frac{W_s - W_d}{W_d} \quad (2)$$

Where W_s and W_d were the weights of the swollen and the dry sample, respectively.

2.3.5. Dynamical mechanical analysis

Dynamical Mechanical Analysis (DMA) was carried out in order to characterize the mechanical behavior of collagen and collagen-nanohydroxyapatite biocomposite scaffolds in wet state under dynamic compression solicitation. Prior to any measurements the samples of approximately 6 mm thickness and 9 mm diameter were immersed in PBS for 1 hour till the swelling equilibrium was obtained. The scaffolds were then subjected to compression cycles of increasing frequencies ranging from 0.1 to 10 Hz at room temperature using a Tritec2000 dynamic mechanical analyser (Triton Tecnology, UK). Three samples were measured for each type of scaffold to obtain the mean values.

2.3.6. *In vitro* degradation analysis

In vitro biodegradation test of the collagen and collagen-nanoHA biocomposite scaffolds was performed by collagenase digestion. Samples of similar weight for each kind of cryogel (~5 mg) were measured dry and immersed in a bath at 37°C with 1 ml of 0.1 M Tris-HCl (pH = 7.4) containing 50 mM $CaCl_2$ for 30 minutes [96]. After 1µl of 0.1 M Tris-HCl containing 50 units of Clostridial Bacterial Type I Collagenase (Sigma-Aldrich, USA) was added to the solution, and the scaffolds were maintained in the bath for more 4 hours. Afterward all the samples were removed and placed in ice with 200 µl of 0.25 M EDTA for 5 minutes [96]. The cryogels were then washed in ethanol in a sequential manner (70 % v/v, 80 % v/v and 90 % v/v) for 10 minutes each, and finally maintained in 100 % v/v ethanol over a period of 1 hour. The samples were subsequently dried inside a laminar flow cabinet for 24 hours and the degree of degradation (D.D) was determined by dry weight change:

$$D.D\ (\%) = 100 \times (W_1 - W_2/W_1) \quad (3)$$

Where W_1 and W_2 are the weights of the initial dry sample before collagenase addition and of the final dried sample after enzymatic degradation, respectively.

2.3.7. *In vitro* biological studies

Cell Culture

Collagen and collagen-nanoHA sections with 0.9 mm diameter and 2 mm thickness were sterilized using ethylene oxide gas. Osteoblast-like cells (MG63, ATCC) were cultured in Eagle minimum essential medium, alpha modification (α-MEM, Sigma) supplemented with 10 % v/v fetal bovine serum (FBS, Gibco), 1 % penicillin-streptomycin (3 x 10^{-4} mol/L and 5 x 10^{-4} mol/L, Gibco) and maintained at 37 °C and 5 % v/v of carbon dioxide (CO_2). After 90% cell confluence in T flasks (75cm^2, Nunc), cells were washed with PBS solution, detached with trypsin solution (0.5 %, Gibco) at 37 °C for 5 minutes and

counted using a Neubauer chamber. Previously to the cell seeding, samples were incubated with complete medium for 1 hour at 37°C in a humidified atmosphere and 5% v/v CO_2. Afterwords, cells were seeded on the collagen and collagen-nanoHA scaffolds (5×10^5 cells/scaffold). The culture medium was changed every 3 days. The time points were evaluated at 1, 7, 14 and 21 days.

Confocal laser scanning microscope

The samples were fixed with 4% w/v paraformaldehyde (Sigma) for 30 minutes and then washed twice in PBS. Then, the materials were incubated for 5 minutes with 0.1 % v/v Triton X100 solution (Sigma), washed twice with 1% w/v bovine serum albumin solution in PBS (BSA, Sigma) and the cytoskeleton were stained with alexafluor-conjugated phalloidin 594 (Invitrogen) at 2.5 % v/v in 1 % w/v BSA solution for 1 hour at room temperature. Samples were washed twice with BSA 1 % w/v and nuclei were stained with DAPI (4'-6-diamidine-2-phenylindole at 0.2 % w/v, Invitrogen) for 5 minutes. Finally the scaffolds were washed twice with PBS and images were acquired with a Leica SP2 AOBS SE camera, with the excitation laser of 358 nm and 594 nm.

Scanning Electron Microscopy

Samples were fixed as described before. Afterwords, they were dehydrated in a sequence of ethanol (50 % v/v to 100 % v/v) and fixed with 1,1,1,3,3,3 – Hexamethyldisilazane, 98% (Acros Organics, Belgium) at an increasing sequence. Subsequently, the materials were allowed to dry on a Petri dish inside the laminar flow cabinet overnight. Samples were fixed onto aluminium sample holders with Araldite™ glue and then sputter-coated with palladium-gold (Bal–Tec–SCD 050) and observed using a scanning electron microscope (SEM, FEI Quanta 400FEG).

DNA extraction assay

DNA content was measured using the Quant-iT^{TM} Picogreen$^{®}$ DNA assay (Invitogen, UK) according to the manufacturer's instructions. Briefly, after the scaffolds were washed with PBS, they were placed at 37 °C and 5 % v/v CO_2 for 1 hour with 1 ml of ultra pure water. Subsequently, they were placed in a freezer at -80 °C for 1 hour and then thawed at room temperature to lyse all the cells membranes cultured inside the materials. Finally the fluorescence intensity was measured with a microplate spectrofluorometer (BioTek) at 530 nm and 590 nm for excitation and emission, respectively**.**

Alkaline Phosphatase Activity and Protein Content

After the time points, samples of collagen and collagen-nanoHA biocomposite scaffolds were washed twice with PBS and prepared as described in the previous item. Afterwords, the thawed cryogels were vortex for 5 seconds and centrifuged (Centrifuge 2-16PK, Sigma) at 10000 rpm for 2 minutes. The enzyme activity was assayed by the substrate hydrolysis, *p*-nitrophenol phosphate (Sigma), in alkaline buffer solution, 2-amino-2-methyl-1-propanol (Sigma), at pH 10.5. After 1 hour incubation at 37°C, the reaction was stopped by adding NaOH (1M, Sigma) and the product (*p*-nitrophenol) was quantified by absorbance measurements at 405 nm, using a plate reader (BioTek). The ALP activity results were normalized to total protein content and were expressed in nanomoles of *p*-nitrophenol produced per minute per microgram of protein.

Total protein content was measured by Lowry's method with bovine serum albumin used as standard.

2.3.8. Histological Analysis

The scaffolds after 21 days of cell culture were washed twice with PBS and placed in ethanol 70% v/v for 24 hours. Subsequently, 3D samples were placed in cassettes, dehydrated in graded ethanol (70% v/v, 80% v/v, 90% v/v and 100% v/v) and then immersed in xylene 100% v/v (Sigma). Samples were then immersed in infiltration medium paraffin (Leica) twice for 30 minutes and then embedded in paraffin. Samples were left to dry for 30 minutes at room temperature. Paraffin embedded disk specimens were later cut with a microtome (Leica) at a thickness of 3 µm. After deparaffinization and dehydration, the sections were stained with hematoxylin (Surgipath) and eosin (Aldrich) (H&E) for examination. Samples were then observed with a light microscope (Olympus light microscope).

Statistical Analysis

Data were presented as mean ± standard deviation ($n = 3$) and analyzed using the one way ANOVA test. Differences between groups were considered statistically different when $p < 0.05$.

Chapter III

Results

Results

3.1. Scanning Electron Microscopy

Samples morphology and porosity were analyzed by scanning electron microscopy. Figure 14 showed the SEM images of collagen and collagen-nanoHA biocomposite scaffolds. The scanning electron micrographs showed the sponges with heteroporous morphology and with a highly interconnected three-dimensional structure.

In the case of composite scaffolds, the nanoHA aggregates were homogeneously dispersed and strongly adhered throughout the collagen structure. As expected, the quantity of nanoHA aggregates in the scaffold decreased with the decrease of their concentration in the initial suspension.

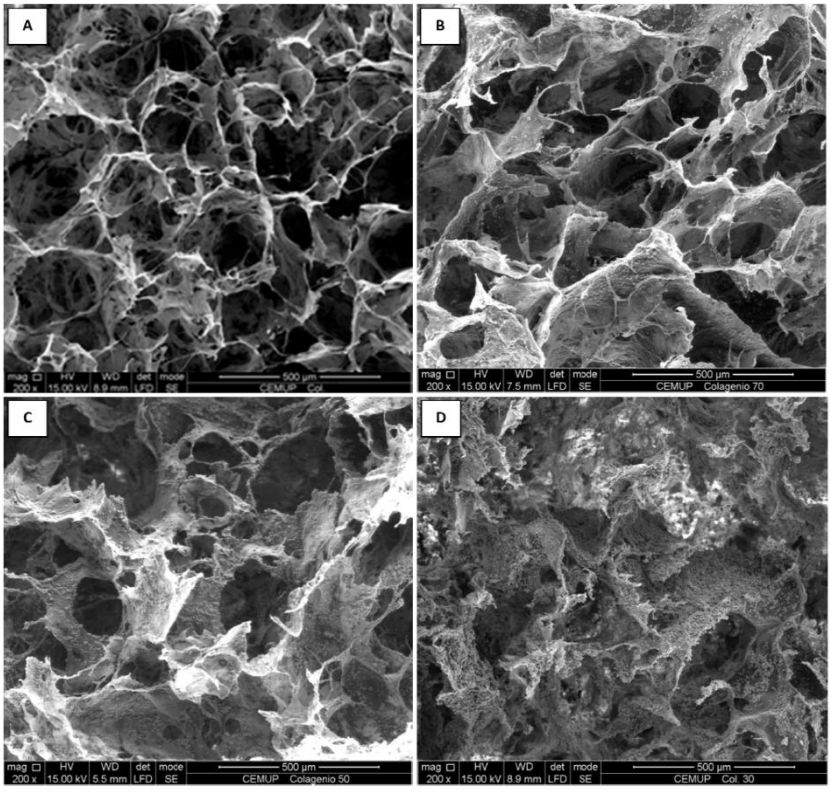

Figure 14. Scanning electron micrographs (SEM) of the cross-sections of (A) collagen scaffold (B) collagen-nanoHA (70:30) scaffold, (C) collagen-nanoHA (50:50) scaffold and (D) collagen-nanoHA (30:70) scaffold. Magnification: x 200.

SEM images did not only allow us to acquire qualitative information about the scaffolds but also allowed the porosity assessment, by analyzing the images with ImageJ software. Pores sizes between 10 and 350 µm were measured by the software, with an average pore size of 83.14 ± 45.88 µm for collagen scaffold, 84.12 ± 62.42 µm for collagen-nanoHA (70:30) scaffold, 58.59 ± 39.91 µm for collagen-nanoHA (50:50) scaffold and 54.82 ± 32.24 µm for collagen-nanoHA (30:70) scaffold (Tab. 1).

Table 1. Average, maximum and minimum pore diameter (µm) of collagen and collagen-nanoHA biocomposite cryogels.

Characteristics	Cryogels			
	Collagen	Coll-nanoHA (70:30)	Coll-nanoHA (50:50)	Coll-nanoHA (30:70)
Average pore diameter	83.48 ± 45.88	84.12 ± 62.42	58.59 ± 39.91	54.82 ± 32.24
Maximum pore diameter (µm)	288.79	339.23	265.82	207.28
Minimum pore diameter (µm)	21.42	14.89	12.36	11.51

Pore size distributions in all the scaffolds are represented in Figure 15. All the samples showed a very heterogeneous structure (such as observed by SEM images) with higher percentage of pores between 10 and 170 µm of size. However, collagen-nanoHA (70:30) cryogel had higher number of pores over 200 µm when compared with the other scaffolds. The collagen-nanoHA (30:70) composite did not show pores over 210 µm (Fig.15).

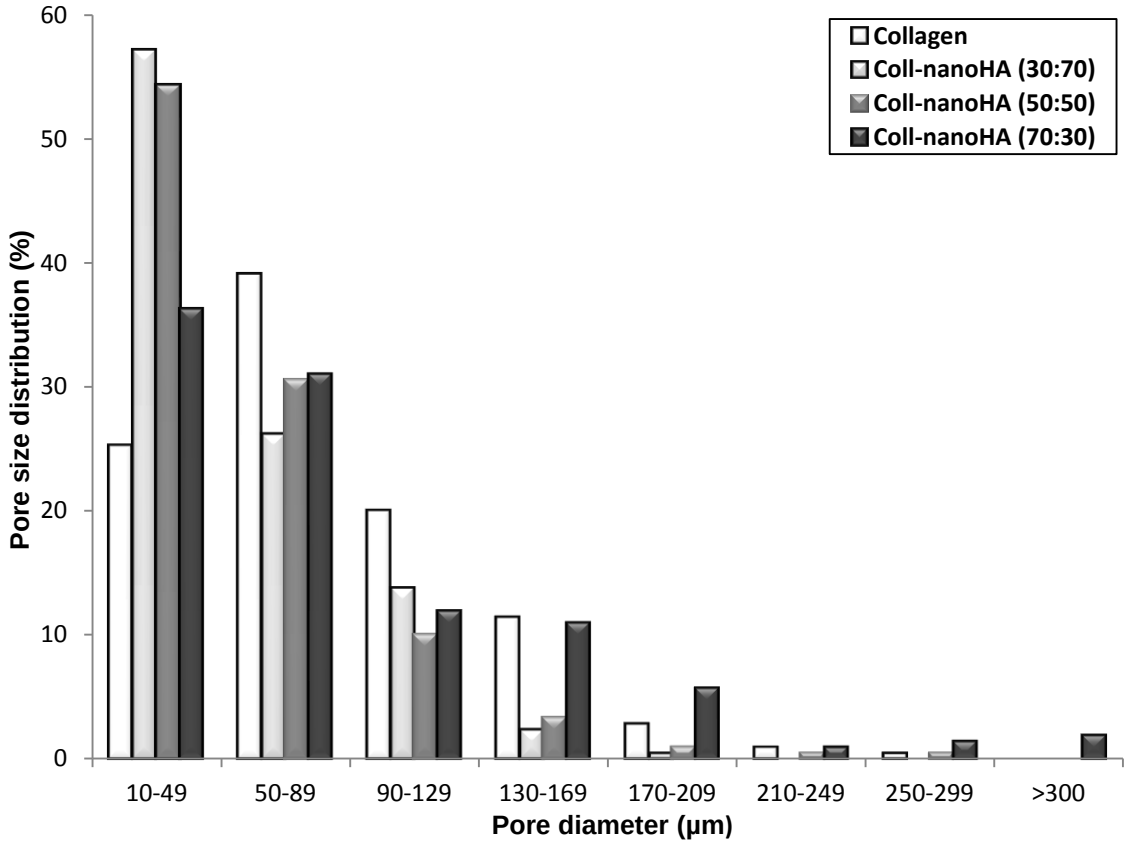

Figure 15. Pore distribution for collagen and collagen-nanoHA biocomposite scaffolds.

3.2. FTIR

The FTIR spectra of collagen and collagen-nanoHA biocomposite scaffolds are represented in Figure 16. The spectrum of collagen scaffold (Fig. 16A) exhibited typical amide bands of proteins i.e. 1658 cm^{-1} was ascribed to amide I (C=O stretching), 1550 cm^{-1} to amide II (N-H deformation) and 1239 cm^{-1} to amide III (N-H deformation) [97]. Similarly, the spectrum of pure nanoHA aggregates (Fig. 16E) represented typical peaks of hydroxyapatite. The bands at 1031, 962, 602 and 564 cm^{-1} were due to the molecular vibrations of phosphate group (PO_4^{3-}) presented in nanoHA aggregates. The 1031 and 962 cm^{-1} bands corresponded to v3 and v1 mode vibration of PO_4^{3-}, whereas bands at 602 and 564 cm^{-1} were due to v4 mode vibration of PO_4^{3-}. The band of carbonate (CO_3^{-}) appeared at 875 cm^{-1} (v2 vibration) [97, 98]. The spectra of collagen-nanoHA biocomposite scaffolds (Fig. 16B, C, D) showed all major

bands of collagen as well as the peaks for hydroxyapatite. In case of composite scaffolds the amide I band appeared at 1648 cm^{-1}.

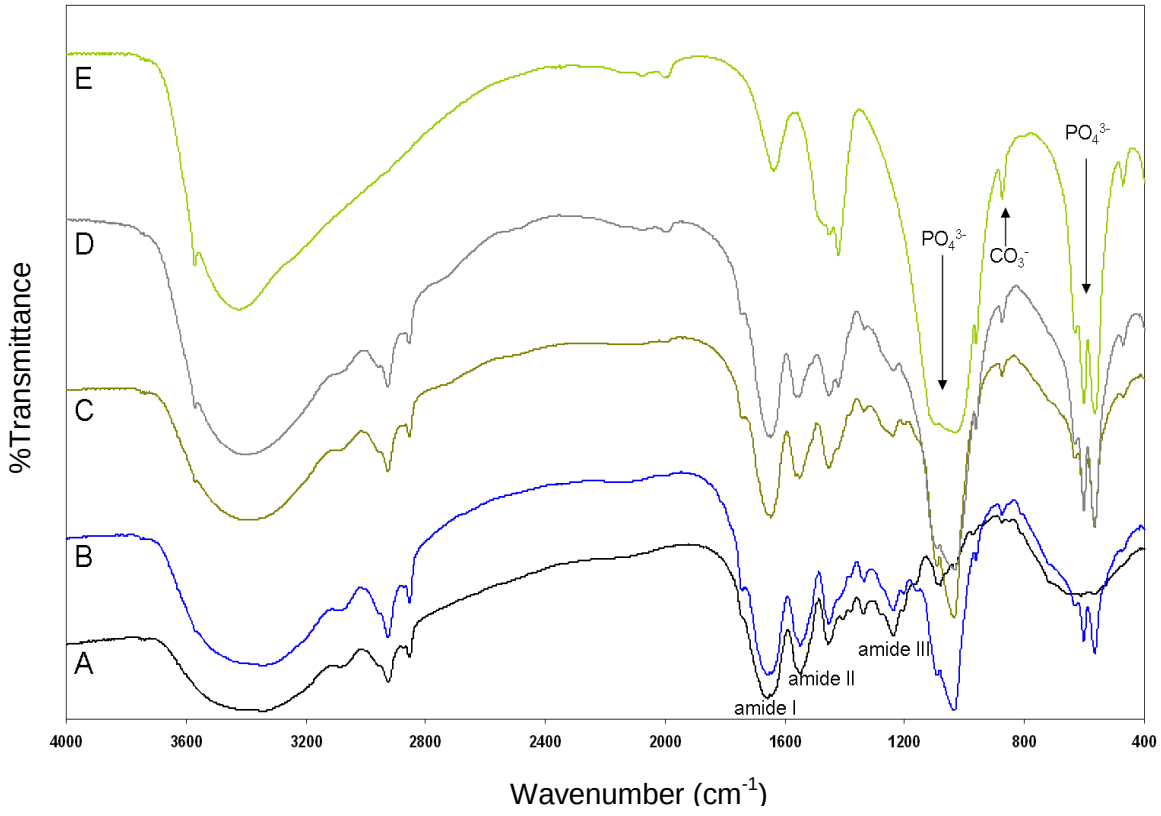

Figure 16. FTIR spectra of (A) collagen scaffold, (B) collagen-nanoHA (70:30) scaffold, (C) collagen-nanoHA (50:50) scaffold, (D) collagen-nanoHA (30:70) scaffold and (E) nanoHA aggregates.

3.3. Mercury Intrusion Porosimetry

Mercury intrusion porosimetry results showed that the collagen-nanoHA (30:70) scaffold presented higher surface area than the other samples (Tab. 2). Total porosity volume was also higher for collagen-nanoHA (30:70) followed by the collagen-nanoHA (50:50) and the collagen-nanoHA (70:30) (Tab. 2). Furthermore, it was possible to observe that total surface area as well as total porosity volume increased as nanoHA content increased in the scaffold. As the mercury intrusion accounted only for pore diameters in the range of 0.004-15.04 µm, larger pores diameters were determined by SEM images, as previously discussed.

Table 2. Results obtained from mercury intrusion porosimetry for collagen-nanoHA biocomposite scaffolds.

Cryogels	Surface area (m^2/g)	Theorical porosity (%)	Apparent Density (g/cm^3)
Coll-nanoHA (70:30)	0.53	93.83	0.08
Coll-nanoHA (50:50)	36.63	96.32	0.06
Coll-nanoHA (30:70)	55.44	96.65	0.08

3.4. Swelling Properties Test

The water-binding ability of the scaffolds is an important feature to evaluate the capability to be applied in tissue engineering [99]. Figure 17A and Figure 17B show the swelling behavior of collagen and of different collagen-nanoHA biocomposite scaffolds in PBS and water, respectively. The water uptake sharply increased at the initial stage, and then reached the equilibrium swelling after approximately 15 minutes. It was also possible to observe that with the impregnation of nanoHA into the polymer matrix, there was an important modification on the water absorption behavior. The results clearly revealed that the swelling ratio continually decreased as nanoHA content increased in the composite.

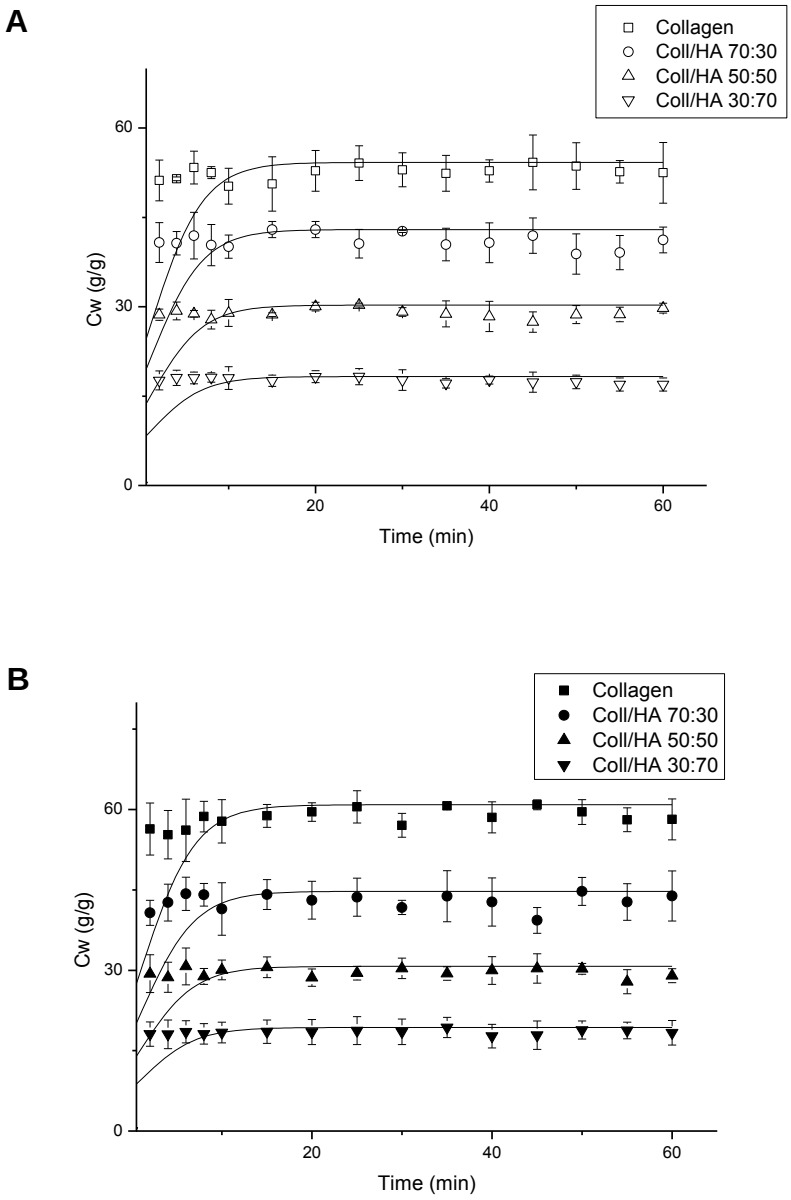

Figure 17. Swelling kinetics of collagen and collagen-nanoHA biocomposite scaffolds in PBS buffer (A) and distilled water (B). Swelling data were fitted to the Boltzman Model.

3.5. Dynamical Mechanical Analysis

In order to approach the *in vivo* condition, a mechanical test with swollen scaffolds was performed. Figure 18 represents the viscoelastic behavior of the collagen and collagen-nanoHA biocomposite scaffolds. Figure 18A shows the variation of the storage modulus (E') with the frequency scan (from 0.1 to 10 Hz). The storage modulus represents the elastic component of a material and it was an indicator of the capability of a material to store energy during deformation [100]. As it may be seen, E' increased with increasing nanoHA content in the scaffold. Figure 18B shows the variation of loss factor (tanδ) with the frequency. The loss factor is the ratio between the amount of energy dissipated by viscous mechanisms and the energy stored in the elastic component, providing information about the viscoelastic properties of the material [101]. For all the scaffolds, tanδ increased with the enhancement of the frequency. However, it was possible to observe that the inclusion of nanoHA in the collagen scaffold decreased the loss factor.

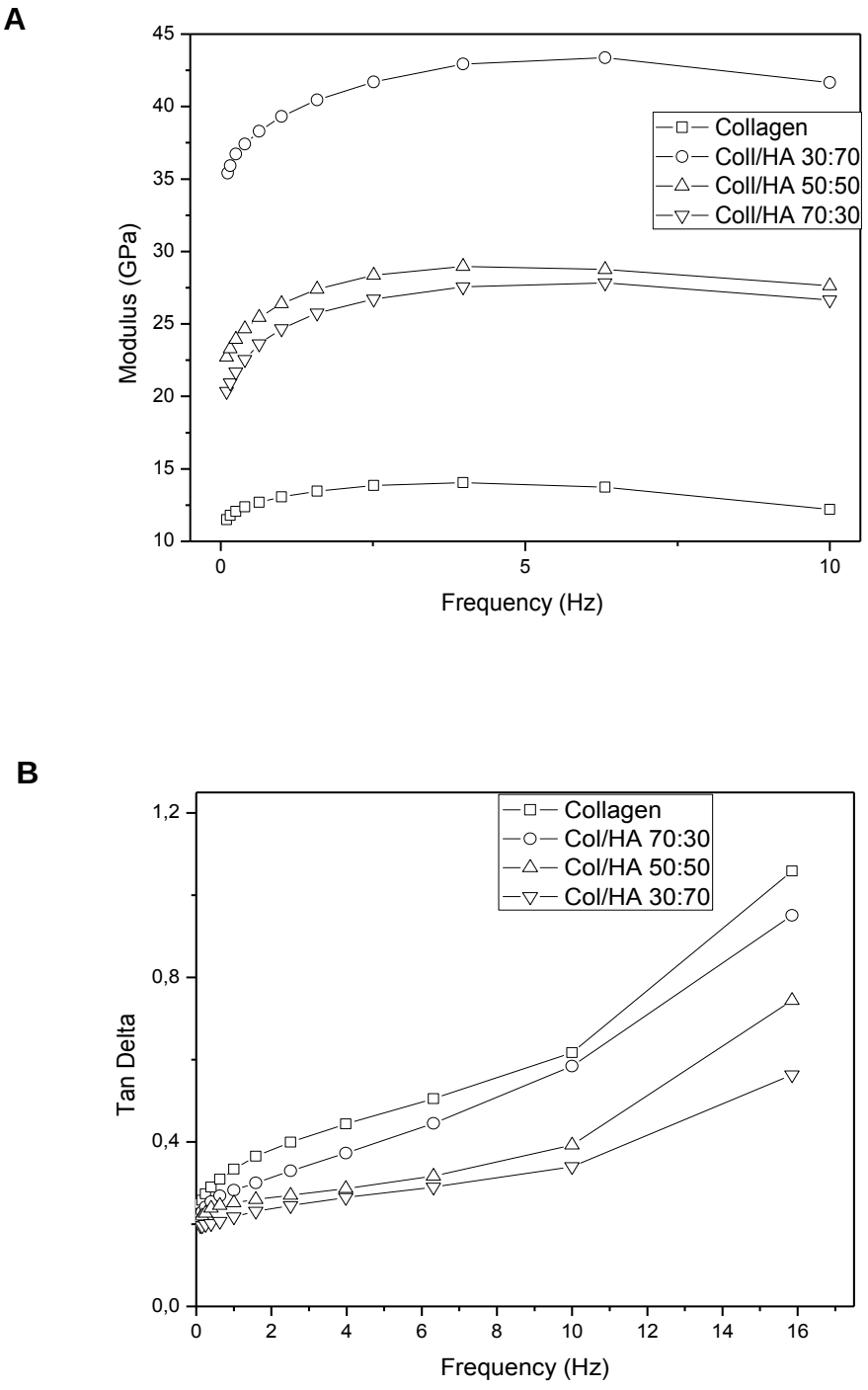

Figure 18. Storage modulus (A) and loss factor (B) under dynamic compression solicitation versus increasing frequency, ranging from 0.1 to 10HZ.

3.6. *In vitro* degradation analysis

Another important factor for scaffolds when designing temporary or long-term implants for tissue engineering is their biodegradability. Collagenase (Type I) is an enzyme released by osteoclasts in order to breakdown the collagenous network in bones. Collagenase binds to triple helices, and degrades collagen starting from the surface [102]. In order to partially mimic the *in vivo* biodegradation conditions, samples were placed in collagenase environment at body temperature. The degree of scaffolds degradation was determined by the change in dry weight of the test samples. All the cryogels degraded and the degree of degradation of collagen and collagen-nanoHA biocomposite scaffolds was represented in Figure 19. The results revealed that the composite degradation rate was higher when compared to the collagen scaffold and the degree of degradation tended to increase as the nanoHA content increase in the polymer matrix. However, differences between collagen and collagen-nanoHA biocomposite scaffolds were not statistically significant.

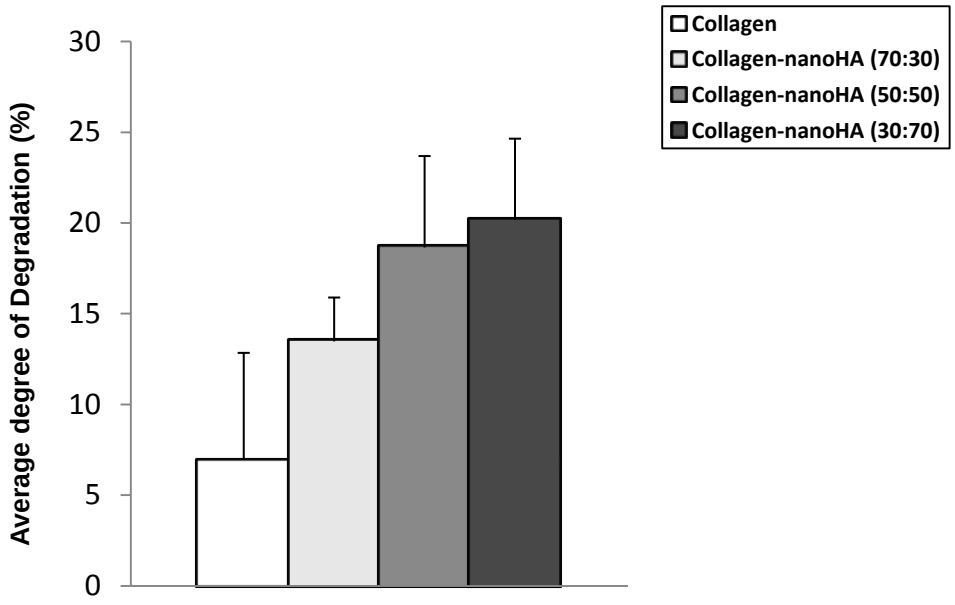

Figure 19. Average degree of degradation of collagen and collagen-nanoHA biocomposite scaffolds**.**

3.7. *In vitro* biological studies

When the cells are in contact with the biomaterials' surface, they should have some morphological modification in order to stabilize the cell-matrix interface. The most important events of cell attachment include cell adhesion to the substrate, radial growth of filopodia, cytoplasmatic networking and flattening of the cell mass progressing in a sequential manner [103]. SEM images of MG63 cells seeded on collagen and collagen-nanoHA biocomposite scaffolds were obtained to observe the cell biocompatibility behavior (Fig. 20). At day 7 of culture, it was observed that the cells presenting a spindle-like morphology were well attached to the collagen sample, although they did not spread (Fig. 20A), while on collagen-nanoHA scaffolds they were well adhered and spread out (Fig. 20D, G and J). Moreover, it was observed that the cells cultured on biocomposite cryogels were well flattened, exhibiting numerous filopodial-like extensions and cell-to-cell contact points. At day 14, biocomposite scaffolds surface and macropores access were almost completely covered by the cells that formed continuous cell layers in some regions. However, in the collagen scaffold the cells were aggregated to each other presenting a round shape (Fig. 20B with an arrow signed). Finally, at day 21 the biocomposite scaffolds were completely covered by cell layers, while the collagen scaffolds only presented a small part of their surfaces covered by cells (Fig. 20C with an arrow signed). No cytotoxicity responses were observed for any of the evaluated samples. At higher magnifications the cells presented rough dorsal surfaces, characteristic of active cells.

The cells distribution on collagen and collagen-nanoHA biocomposite scaffolds was also observed using confocal laser scanning microscope. CLSM images (Fig. 21) show that the cells were well spread out in all the samples and entirely covered the surface of collagen-nanoHA scaffolds, a result similar to those observed by SEM. CLSM images also confirmed that collagen scaffold seem to have fewer cells when compared to composite cryogels. Furthermore it was possible to observe that cells were able to orient their growth according to the materials' surface morphology.

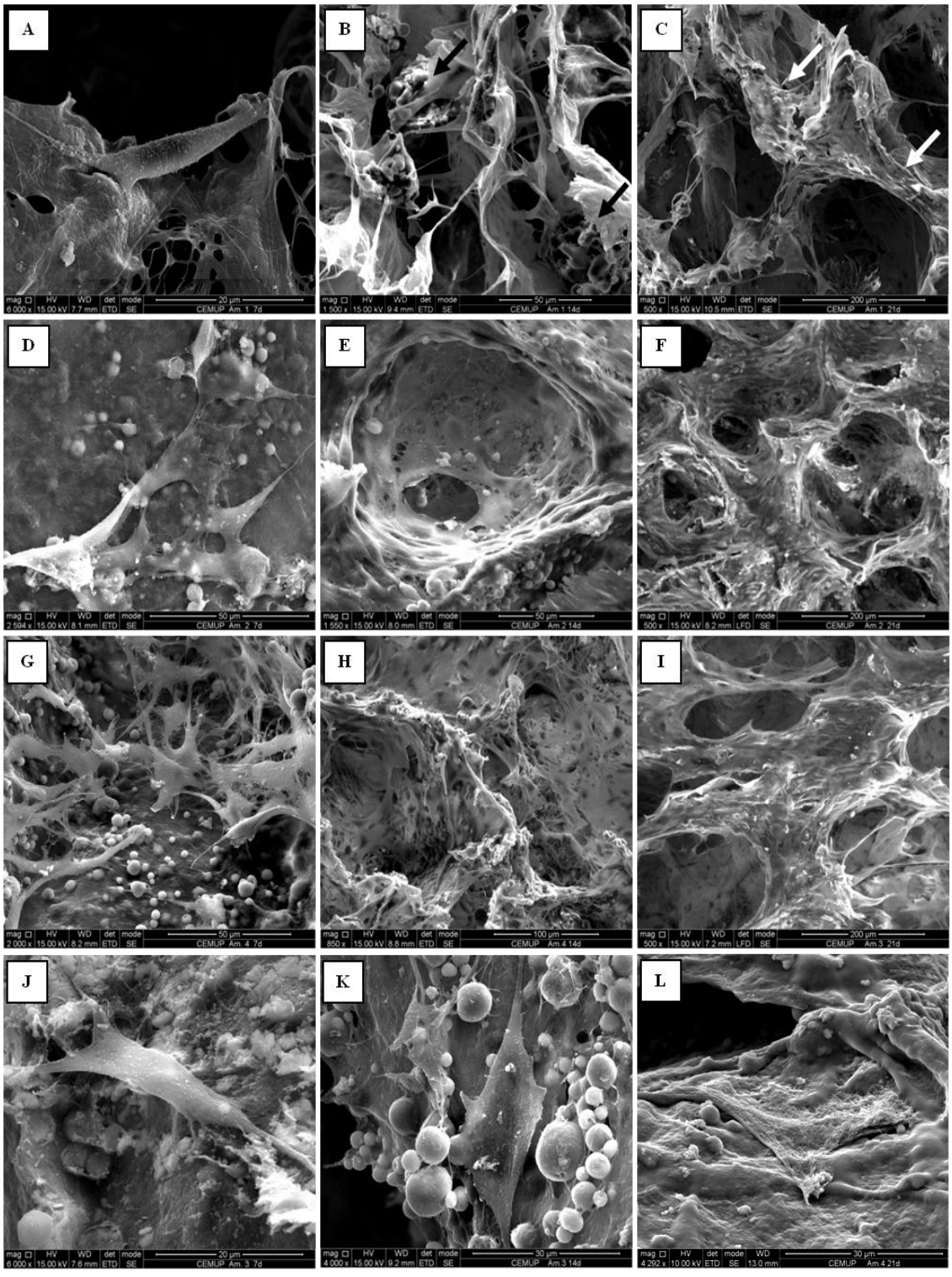

Figure 20. SEM images of osteoblast-like MG63 cells cultured on cryogels' samples (A, B and C – collagen; D, E and F – collagen-nanoHA (70:30); G, H and I - collagen-nanoHA (50:50);J, K and L - collagen-nanoHA (30:70), after 7 days (A, D, G and J), 14 days (B, E, H, and K) and 21 days (C, F, I and L).

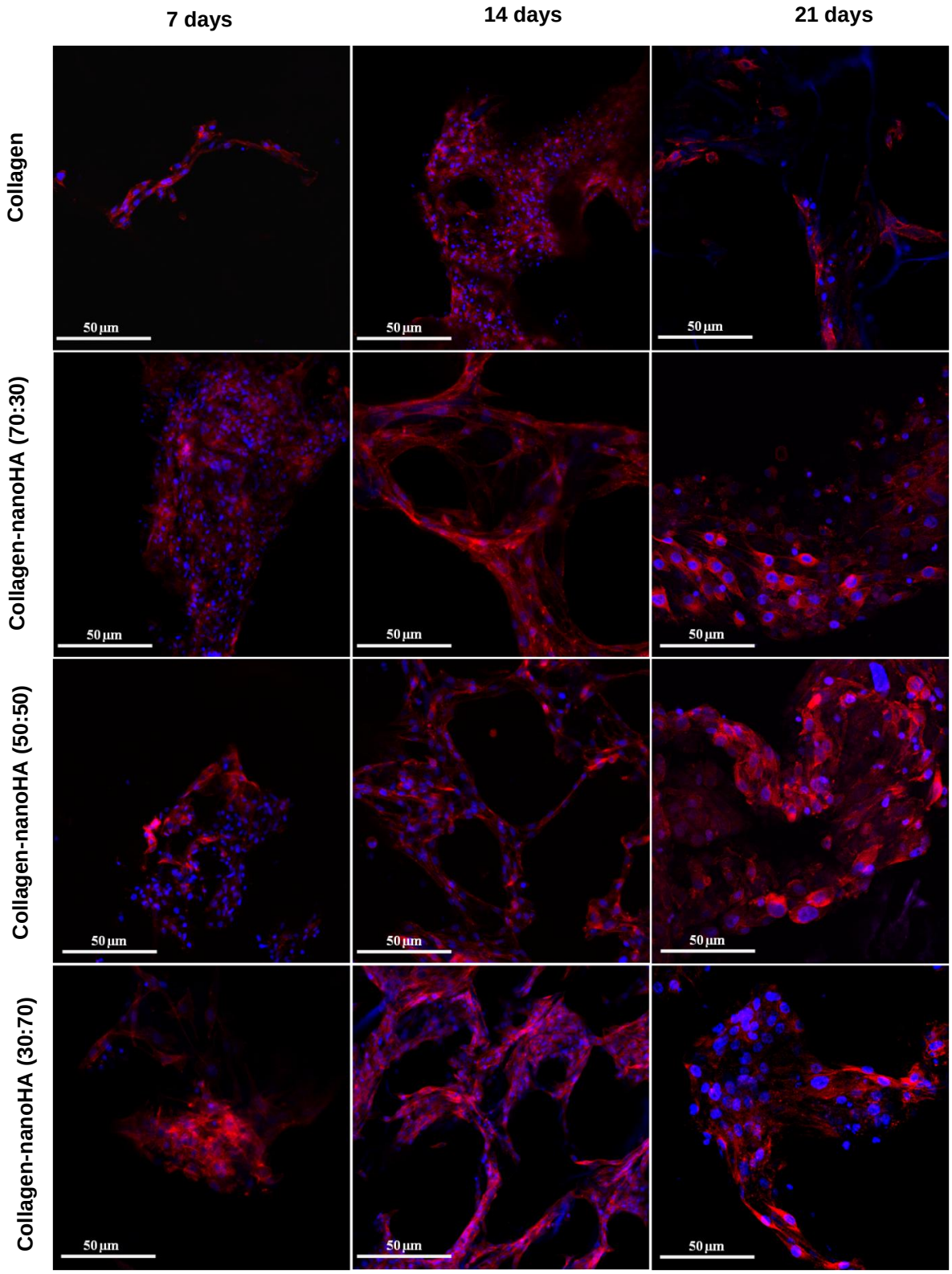

Figure 21. CLSM images of cells cultured for 7, 14 and 21 days on collagen and collagen-nanoHA biocomposite scaffolds. Cytoskeleton is indicated in red while cell nuclei were stained in blue.

Cell proliferation, estimated by DNA extraction quantification, is shown in Figure 22. It was possible to observe that collagen-nanoHA biocomposite scaffolds resulted in higher overall proliferation compared to the collagen cryogel. Moreover, the total DNA content at 21 day of culture in collagen-nanoHA sponges was significantly higher than those in the collagen samples.

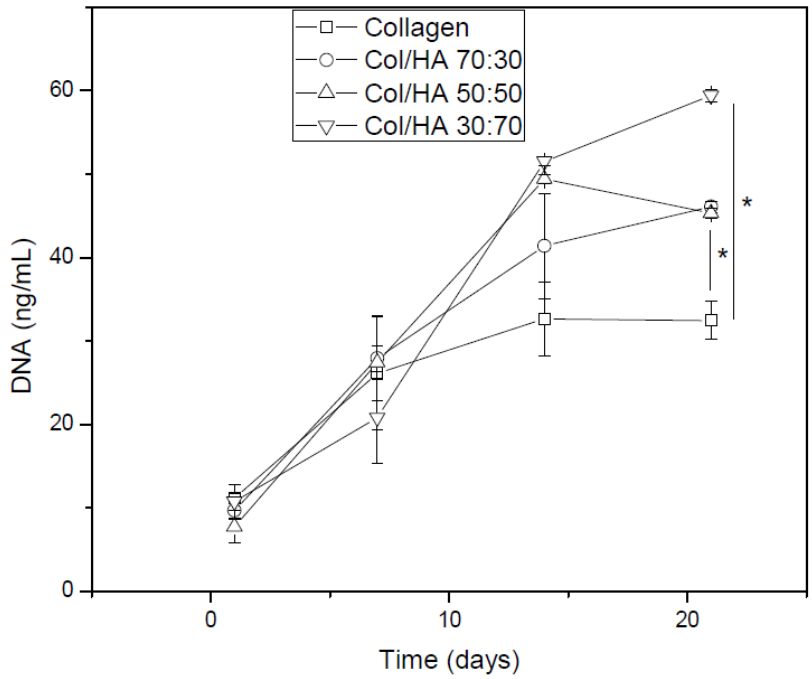

Figure 22. Total DNA extraction quantification of MG63 cells seeded on collagen and collagen-nanoHA biocomposite scaffolds. Differences between collagen and biocomposite scaffolds were statistically significant ($\boldsymbol{p} < 0.05$).

The functional activity of the cells on the collagen and collagen-nanoHA biocomposite scaffolds was assessed by measuring the ALP activity by the cells after culturing for up to 21 days. ALP is a common indicator of the expression of the osteoblastic phenotype [104]. ALP produced by MG63 osteoblast-like cells was normalized with total protein measurement and the results were expressed in nmol/min/µg, as shown in Figure 23. Although the ALP activity tended to be higher in the biocomposite scaffolds than in the collagen cryogel at 1, 7 and 21 days, the difference was not statistically significant. However, at day 14, the

cells in collagen-nanoHA (50:50) and collagen-nanoHA (30:70) biocomposite scaffolds exhibited significantly higher ALP levels than those in the control cryogel. A down-regulation was observed from day 14 to day 21 for all the cryogel scaffolds.

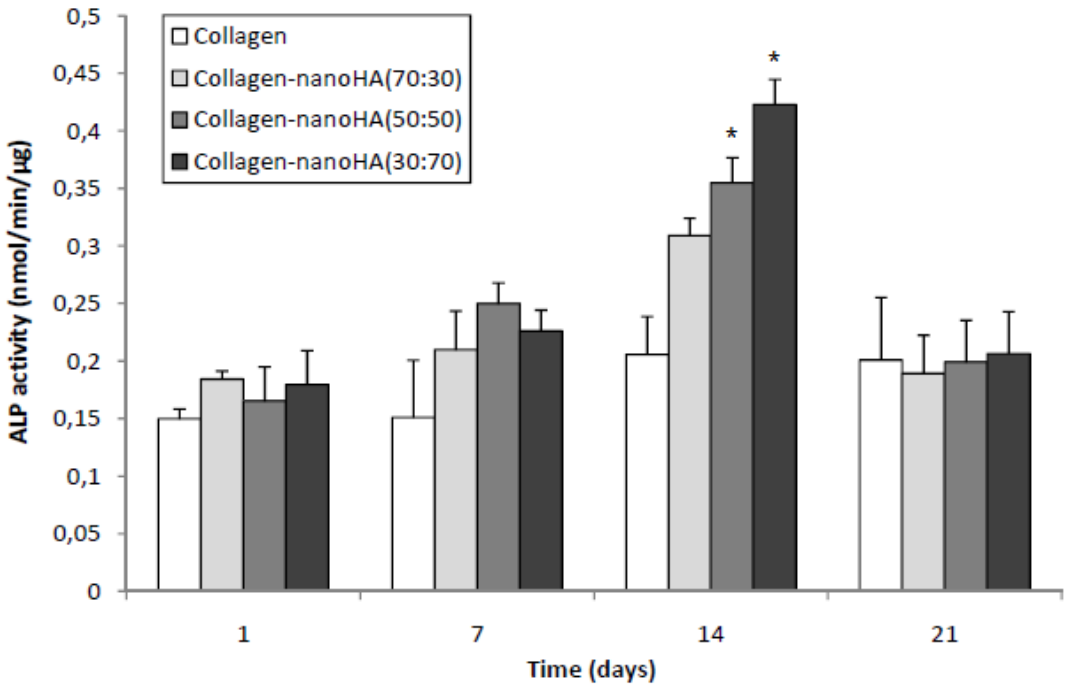

Figure 23. Alkaline phosphatase activity for osteoblastic phenotype expression of MG63 osteoblast-like cells cultured on collagen and collagen-nanoHA biocomposite scaffolds for different time points. Differences between collagen and biocomposite scaffolds were statistically significant ($\boldsymbol{p} < 0.05$).

3.8. Histological Analysis

Slides of transverse sections of samples' surface were histological prepared and stained with Hematoxylin and Eosin (H&E). H&E method is the more commonly used in histological analysis, since it exposes the general architecture of tissue [105]. The hematoxylin (blue) stains the cell nuclei and other negatively charged structures while the eosin (pink) stains cell cytoplasm and most connective fibers (i.e. collagen).

Histological examination of the cell-seeded scaffolds using hematoxylin-eosin staining indicated a uniform distribution after *in vitro* culture of osteoblast-like cells on the collagen and collagen-nanoHA biocomposite scaffolds (Fig. 24). For this culture time, cells were observed proliferating into layers on the scaffolds surface presenting fibroblast morphology and were able to orient their growth according to surface morphology. However, the collagen scaffold (Fig. 24A) showed lower cell density when compared with the biocomposite cryogels (Fig. 24B, C and D). These results were consistent with those obtained by DNA extraction assay.

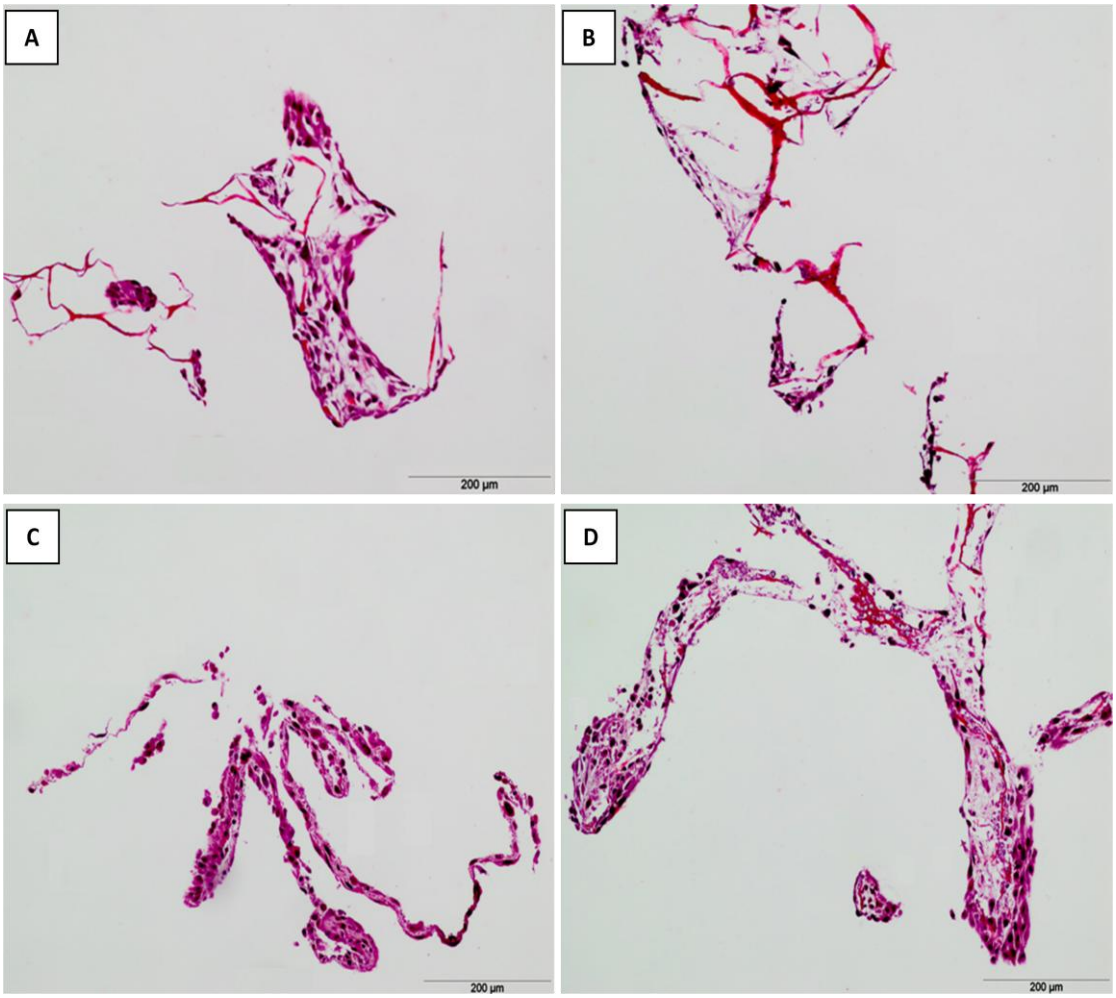

Figure 24. Optical micrographs of stained scaffold sections after 21 days of cell culture. (A) Collagen scaffold; (B) Collagen-nanoHA (70:30) scaffold; (C) Collagen-nanoHA (50:50) scaffold; (D) Collagen-nanoHA (30:70) scaffold.

Chapter IV

Discussion

Discussion

This thesis proposed the development of new bone repair scaffolds prepared by cryogelation method. This technique used ice crystals as templates to produce porous structures without the involvement of organic solvents or any additives during the production, thus rendering this as a favorable process compared with others, currently used to obtain macroporous scaffolds. Since the combination of hydroxyapatite and collagen was shown to be beneficial for bone tissue engineering due to their natural biological resemblance and properties similarity to natural bone [28], three different collagen-nanoHA biocomposite cryogels were obtained and the subsequent morphological, chemical, physical and biological characterizations were performed using several techniques. A pure collagen scaffold was used as a control.

Samples surface analysis by SEM showed that heteroporous morphology was obtained for all sponges. As described for cryogelation [71, 72], the crystallization of the solvent (water) during freezing leads the collagen and EDC/NHS to stay in unfrozen liquid microphase forming the crosslinks. After thawing, pores with variable size and geometry were presented in the bulk cryogel. These cryogels also showed a highly interconnected three-dimensional structure. High pores interconnectivity was desired to enhance the nutrients and metabolites diffusion inside the scaffold [49]. Moreover, for collagen-nanoHA biocomposite scaffolds, the nanoHA aggregates were strongly adhered throughout the collagen structure. These particles adhesion was very important because particles detachment could cause significant problems, i.e., free particles could migrate from the scaffold and could induce an inflammatory response in the body; therefore they should never be released or be rapidly dissolved [106].

SEM analysis revealed the majority of the pores of the collagen and collagen-nanoHA cryogel scaffolds lying in the range of 10-170 µm, while pore diameters as measured by mercury intrusion porosimetry was in the range of 0.004-15.04 µm. It has been reported that the ideal scaffold must exhibit both

microporous and macroporous structure [107-109]. Pores size below 10 µm could be essential for cell-matrix interactions, transfer of nutrients and metabolites and pores size above 100 µm are required for *in vivo* bone ingrowth into the scaffold materials [107, 108, 110]. Previous studies showed that pore size was also critical for vascular ingrowths in a porous scaffold, thus pores above 140 µm diameter were more appropriate to obtain adequate angiogenesis [111]. As a result, pore size is a decisive factor in the use of the materials as scaffolds for tissue engineering. The cryogel scaffolds produced in this work fulfilled these requirements, taking into account that larger pores could compromise mechanical stability of these materials. In addition, pore size of the scaffolds produced in this study is in agreement with pore size of other cryogel scaffolds obtained in previous studies using the same production method. Tripathi *et al* [81] prepared chitosan-gelatin scaffolds by cryogelation method and obtained cryogels with a well interconnected porous structure with pores sizes in the range of 30-100 µm. Mu *et al* [112] synthesized collagen cryogels crosslinked by dialdehyde starch with pore diameters between 20 and 200 µm. Bloch *et al* [80] prepared agarose-gelatin cryogel scaffolds with a pore size between 50-250 µm. However, our cryogel scaffolds presented a better microporosity, since we obtained pores sizes below 10 µm.

Regarding FTIR analysis, the presence of all major peaks related to collagen and hydroxyapatite was observed, whose wavelengths are in accordance with the literature [97, 98]. There are only a few papers published so far regarding collagen/hydroxyapatite composites preparation and it is believed that chemical interaction between hydroxyapatite and collagen can be evaluated from the infrared spectrum of collagen/hydroxyapatite composite [28, 113]. The infrared spectrum analysis of the collagen-nanoHA biocomposite scaffolds synthesized in the present study revealed the amide I band with a slight shift in its wavelength. Similarly, Sionkowska and Kozlowska [28] that characterized collagen/hydroxyapatite composite sponges and studied their potential as bone substitutes also observed that the FTIR spectra showed a shift of the amide I band when they added hydroxyapatite to the collagen matrix. The amide I band represented stretching vibration of C=O and the displacement

of the band probably represented the interaction of Ca^{2+} from nanoHA with collagen [97]. This suggested that some nanoHA aggregates could be linked to collagen surface through the interaction of carbonyl groups [28, 97].

Considering the mercury intrusion porosimetry results, total surface area increased as the nanoHA content increased in the materials' structure. This result was expected due to the inclusion of the nanoHA aggregates with large specific surface area in the collagen matrix. Chesnutt *et al* [114] that prepared chitosan/nanocrystalline calcium phosphate (CaP) composite and a plain chitosan scaffolds, having observed that the composites were rougher and, as a result, had 20-fold larger specific surface area than pure chitosan scaffolds. Similarly, Ngiam *et al* [115] prepared nanoHA/PLGA/collagen composite and PLGA/collagen scaffolds also observed that nanoHA/PLGA/collagen scaffolds had a higher surface area than PLGA/collagen scaffolds.

Porosity is another important characteristic for an ideal scaffold to be used in tissue engineering applications as high levels of porosity play a critical role in *in vitro* and *in vivo* bone formation [116]. All the synthesized cryogel scaffolds showed high porosity over 90%, which was considered to be beneficial for cell ingrowth and survival.

The water-binding ability of the scaffolds is another important feature to evaluate their capability to be applied in tissue engineering. Swelling facilitates the cells infiltration into the scaffolds in a three-dimensional scaffold, during cell culture [117]. Swelling also increases the pore size thus maximizing the internal surface area of the scaffolds [117]. Samples showing higher degree of swelling will have a larger surface area/volume ratio, thus allowing the samples to have the maximum probability of cell infusion into the 3D scaffold [117]. The swelling ability of the scaffolds will help to absorb the culture medium and hence allow the easy passage nutrients through it [117]. However, it is important to note that the swelling of scaffolds may probably decrease their mechanical properties. Hence, controlled swelling will be ideal for tissue engineering applications [117].

Swelling studies of collagen and collagen-nanoHA biocomposite scaffolds indicated very high swelling capacity and the ability to retain more water than their original weight. It was observed that the equilibrium swelling was reached

after approximately 15 minutes. This fast swelling behavior was a characteristic response that has been observed with porous and hydrophilic materials [74]. These materials had presented a large range of interconnected pores that should allow faster transportation of solvent molecules within thin walls over short distances across the scaffold structure. Therefore, interconnectivity of pores plays a crucial role in faster swelling rate of cryogels as the solvent molecules can move by convection across this network, while in the conventional hydrogels this process should depend on the solvent diffusion and therefore should be slower [74]. Another important aspect was the impregnation of nanoHA into the polymer matrix that brought about a significant change in water absorption behavior. The results clearly revealed that the swelling ratio continuously decreased as nanoHA content increased in the composite. Previous studies by Thein-Han and Misra [17] also described a decrease in the degree of water absorption by addition of nanoHA aggregates to chitosan scaffolds. Peter *et al* [118] had observed that chitosan-gelatin/nanohydroxyapatite (CG/nanoHA) composite scaffolds had higher swelling capacity and the ability to retain water; however the addition of nanoHA decreased the swelling rate of CG/nanoHA scaffolds. Similarly, Poursamar *et al* [119] that studied polyvinyl alcohol/hydroxyapatite (PVA/HA) composite had observed that, as the scaffolds had higher HA content, they showed less water uptake when compared with other samples that did not contain this ceramic particle. Therefore, our results followed the same behavior and this may be explained by the fact that due to relatively low hydrophilicity of nanohydroxyapatite particles, its increasing fraction in the composite could result in decreasing solvent absorption by the sample [120]. Moreover, the increase of collagen-hydroxyapatite interactions with higher concentration of nanoHA resulted in a slower relaxation of polymer chains which also decreased the swelling ratio [120].

One of the key issues of scaffolds design for tissue engineering is their mechanical performance. In the case of load-bearing tissues such as bone, the scaffold matrix must provide sufficient temporary mechanical support to withstand *in vivo* stresses and loading [121]. Moreover, the mechanical

properties of the scaffold will influence the mechanical environment of the seeded cells [122]. Therefore, mechanical properties of the scaffold before implantation are key determinants of its eventual long-term success or failure [122]. In the present study, we have evaluated the mechanical performance of collagen and collagen-nanoHA biocomposite scaffolds in hydrated state under dynamic solicitation, therefore mimicking the *in vivo* physiological condition in a post-implantation scenario. The dynamic mechanical behavior of the scaffolds was characterized by DMA and both storage and loss modulus were measured in the frequency range 0.1-10 Hz. An increase of the storage modulus with the increase of nanoHA content in the scaffold was observed, promoting the materials stiffness. As a result, the uniform dispersion of nanoHA within the polymer matrix improved the mechanical properties of the scaffolds. This would be expected as the nanoHA particles reinforced the scaffolds and varying the amount of nanoHA in the composite, a range of the mechanical properties could be obtained [123]. In addition, for all the cryogel scaffolds, the loss modulus increased with the enhancement of the frequency indicating that the specimens became more viscous and less elastic. However, it was possible to observe that the inclusion of nanoHA in the collagen scaffold decreased the loss factor. These findings are supported by the work of Malafaia and Reis [121], who studied bilayered chitosan based scaffolds for osteochondral tissue engineering and also verified that the storage modulus increased and the loss factor decreased on the chitosan scaffolds by incorporating hydroxyapatite in the polymeric matrix. Also, Juhasz *et al* [124] who prepared novel bioactive nano-calcium phosphate-hydrogel composites and studied their mechanical properties also found some benefits in including ceramic nanoparticles in PHEMA/PCL gels, since an improvement on the mechanical properties of these hydrogels was observed.

Ideally, biological scaffolds used in tissue engineering are incorporated *in vivo* by a process of cellular in-growth, followed by host-mediated degradation and replacement of these scaffolds. Therefore, the degradability of the scaffold is very important. An ideal scaffold must possess a degradation rate that closely matches the regeneration rate of the new tissue [125]. Collagenase digestion

can represent an *in vitro* measure of degradation rate for a biological implant [126]. To mimic the *in vivo* conditions as close as possible, all the cryogel scaffolds were placed in collagenase environment at 37°C. All cryogel scaffolds were degraded by collagenase and the presence of hydroxyapatite influenced collagen biodegradability. The degradation of the scaffolds in a collagenase medium is deemed to be closely related to the accessibility of the enzyme to the collagen fibrils [127]. Several works [127, 128] have shown that collagen-nanoHA composites show a significant improvement in its stability against biodegradation mediated by collagenase enzyme. According to these studies the nanoHA aggregates precipitated on the collagen fibrils may inhibit the binding of the enzyme, because the number of exposed collagen molecules is reduced as a consequence of the coverage by apatite component [127,128]. Therefore, increased number of nanoHA aggregates had the highest blocking effect on enzymatic degradation, consequently improving stability [127]. In the present study, this stability against biodegradation was not observed by the biocomposite scaffolds. Instead, it was observed that the composite degradation rate was higher than for pure collagen cryogel and the degree of degradation tended to increase as the nanoHA percentage increased in the polymer matrix. The reason for this is probably related to the fact that the nanoHA aggregates in our biocomposite scaffolds are randomly dispersed throughout the collagen matrix and they are not functioning as a protective coating as in the referred previous work.

For bone tissue engineering, primary osteoblast or secondary cell lines such as human osteoblast-like cells (MG63) are commonly employed as *in vitro* models [129]. According to Kirkpatrick and Mittermayer [130], MG63 cell line provides a useful tool both to investigate the effects of biomaterials and to understand the mechanisms of cell response. As a result, the biological performance of collagen and collagen-nanoHA biocomposite scaffolds was performed by using MG63 cells cultured up to 21 days on the cryogels in order to evaluate cell attachment, spreading and proliferation.

At early culture times, the cells cultured on the biocomposite cryogels were well adherent and spread out, while the cells cultured on the control sample were only able to attach.

For long incubation times, dense multilayers were observed, both on the surface and on the macropores internal surface of the biocomposite scaffolds, and also the presence of cell bridges connecting the macropores was observed. On the collagen sample, only a small part of its surface was covered by cells.

In terms of cell proliferation, it was possible to observe that collagen-nanoHA biocomposite scaffolds resulted in higher overall growth than collagen cryogel. These results were also confirmed by histological analysis because the collagen cryogel showed lower cell density than the biocomposite scaffolds.

The presence of the nanoHA aggregates induced differences in terms of surface roughness between the biocomposite scaffolds and pure collagen scaffold because their presence should induce a rougher surface. This may partially explain the cell behavior results. In the literature it is well known that the behavior of osteoblasts is significantly influenced by the chemical nature and physical characteristics of the material onto which the cells adhere and grow [87]. Regarding surface physical properties, several works have suggested that surface roughness appears to be capable of conditioning many aspects of cell life, including cell adherence, attachment, spreading, growth and differentiation [87,131-133]. Also, Thanaphum *et al* [134] studied human osteoblast-like cell spreading and proliferation on Ti-6Al-4V alloy surfaces with different degrees of roughness and observed higher cells spreading and proliferation on rougher surfaces rather than on the smoother ones.

In addition to all these observations, it was also possible to confirm by CLSM and histological images that cell growth seemed to be guided by surface morphology. This result is in agreement with previous studies referring that cells can orient themselves according to the morphological patterns [135, 136].

Alkaline phosphatase is a common indicator of the osteoblastic phenotype expression. In the present study, it was observed that ALP expression was higher on the biocomposite scaffolds than on the collagen cryogel. This result illustrated the efficacy of the nanoHA aggregates in enhancing the osteoblastic

phenotype expression level. As a result, the biocomposite cryogels improved the functional activity of the bone-derived cells. A previous *in vitro* biological study by Tsai *et al* [137] performed in collagen-hydroxyapatite composite beads using MG63 osteoblast-like cells, also showed that hydroxyapatite increased the ALP activity of osteoblasts. Similarly, Kim *et al* [138] that studied osteoblast responses to gelatin-hydroxyapatite nanocomposites observed that the nanocomposites had significantly higher ALP levels when compared with pure gelatin at day 14 of cell culture. Some studies [139, 140] have indicated that calcium ions are directly involved in enhancing the proliferation and the osteoblast cells phenotype expression by membrane mediated ion transfer, which possibly can explain these results. However, a down-regulation was observed for all cryogel scaffolds from day 14 to day 21. It has been reported that the alkaline phosphatase reaches its maximum in the cell culture when the cells reach confluence, and subsequently decreases [141-143]. Therefore, possibly the cells reached confluence at day 14 of cell culture, which led to the decrease in the levels of ALP at day 21.

In the present study, the collagen-nanoHA (30:70) biocomposite scaffolds stood out for their enhanced morphological, mechanical and biological properties when compared to the other biocomposite scaffolds. However, it is important to notice that choosing the best biocomposite scaffold for bone tissue engineering depends on the intended application. Since bones are subject to the action of forces in carrying out its mechanical functions, mainly mechanical loads must be studied keeping in mind the surrounding environment of the scaffold once placed in an *in vivo* environment. Therefore, the mechanical load of the bone must be taken into account before select the most appropriate biocomposite scaffold to be used in bone tissue engineering.

Chapter V

Conclusions and Future work

Conclusions

In this work, collagen-nanoHA biocomposite scaffolds with different relative mass proportions were produced by cryogelation method. The obtained cryogels were highly porous with interconnected porosity and behaved like sponges. Moreover, they exhibited a bimodal distribution of pore sizes namely microporosity and macroporosity that were indispensable for mass transport and to control the cellular mechanisms. Human osteoblast-like cells were cultured for 21 days and they were attached and spread both on collagen and on the biocomposite scaffolds. However, cell proliferation and osteoblastic phenotype expression level on the biocomposite scaffolds was higher than on the collagen sponges. These results showed that collagen-nanoHA biocomposite scaffolds provided a more adequate environment for cell adhesion and proliferation, improving cell response. The combination of these cell culture results, the improvement on mechanical properties (the soft and elastic nature) and the swelling behavior that favor the mass transport, leads to the conclusion that the collagen-nanoHA biocomposite cryogels are potentially novel candidates as scaffolds for bone tissue engineering applications.

Future work

The work carried out and discussed in the present dissertation used an *in vitro* model based on MG63 osteoblast-like cells. Future studies using newly differentiated cells deriving from osteogenic precursors could complete this study and provide new insight on the effect induced by the collagen-nanoHA biocomposite cryogels.

Although *in vitro* test has given some preliminary guide lines about cell biocompatibility, it is still necessary to obtain a much clear idea about the host tissue response to the biocomposite scaffolds after *in vivo* implantation. The immunological response of the organism is not taken into account when *in vitro* tests are carried out, neither is the neovascularization and the interaction between all types of cells and proteins involved in bone regeneration. Therefore, further studies are required to explore the complex interactions occurring after *in vivo* implantation.

References

[1] Hing KA. Bone repair in the twenty-first century: biology, chemistry or engineering? Philosophical Transactions of the Royal Society of London Series a-Mathematical Physical and Engineering Sciences 2004;362:2821-2850.

[2] Downey PA, Michael SI. Bone Biology and the Clinical Implications for Osteoporosis. Physical Therapy 2006;86:77-91.

[3] Olszta MJ, Cheng XG, Jee SS, Kumar R, Kim YY, Kaufman MJ, et al. Bone structure and formation: A new perspective. Materials Science & Engineering R-Reports 2007;58:77-116.

[4] Webster TJ. Nanotechnology for the regeneration of hard and soft tissues. In: Webster TJ editor. 1st ed, World Scientific Publishing Company, 2007:260p.

[5] Mistry AS, Mikos AG. Tissue engineering strategies for bone regeneration. Regenerative Medicine Ii: Clinical and Preclinical Applications 2005;94:1-22.

[6] Salgado AJ, Coutinho OP, Reis RL. Bone tissue engineering: State of the art and future trends. Macromolecular Bioscience 2004;4:743-765.

[7] Athanasiou KA, Zhu CF, Lanctot DR, Agrawal CM, Wang X. Fundamentals of biomechanics in tissue engineering of bone. Tissue Engineering 2000;6:361-381.

[8] Clarke B. Normal Bone Anatomy and Physiology. Clinical Journal of the American Society of Nephrology 2008;3:S131-S139.

[9] Junqueira LC and Carneiro J. Basic Histology. 10thedition, Mcgraw-Hill companies, 2003, 544p.

[10] Nather A. Bone grafts and bone substitutes: Basic Science And Clinical Applications. In: Nather A, editor, World Scientific Publishing Company, 2005:612p.

[11] Vander AJ. Human physiology: the mechanisms of body function. In: Vander AJ, Sherman J, Luciano D, editors. 7th ed, Mcgraw-Hill companies, 1993:818p.

[12] Phan TCA, Xu J, Zheng MH. Interaction between osteoblast and osteoclast: impact in bone disease. Histology and Histopathology 2004;19:1325-1344.

[13] Martinez-Lemus LA, Sun Z, Trache A, Trzeciakowski JP, Meininger GA. Integrins and regulation of the microcirculation: From arterioles to molecular studies using atomic force microscopy. Microcirculation 2005;12:99-112.

[14] Alberts B JA, Lewis J, Raff M, Roberts K, Walter P. Molecular Biology of the cell. 4th ed, Garland Science 2002:1643p.

[15] Khatiwala CB, Peyton SR, Putnam AJ. Intrinsic mechanical properties of the extracellular matrix affect the behavior of pre-osteoblastic MC3T3-E1 cells. American Journal of Physiology-Cell Physiology 2006;290:C1640-C50.

[16] Simian M, Hirai Y, Navre M, Werb Z, Lochter A, Bissell MJ. The interplay of matrix metalloproteinases, morphogens and growth factors is necessary for branching of mammary epithelial cells. Development 2001;128:3117-3131.

[17] Thein-Han WW, Misra RDK. Biomimetic chitosan-nanohydroxyapatite composite scaffolds for bone tissue engineering. Acta Biomaterialia 2009;5:1182-1197.

[18] Lee CH, Singla A, Lee Y. Biomedical applications of collagen. International Journal of Pharmaceutics 2001;221:1-22.

[19] Andronescu E, Ficai M, Voicu G, Ficai D, Maganu M, Ficai A. Synthesis and characterization of collagen/hydroxyapatite: magnetite composite material for bone cancer treatment. Journal of Materials Science:Materials in Medicine 2010;21:2237-2242.

[20] Barnes CP, Pemble CW, Brand DD, Simpson DG, Bowlin GL. Cross-linking electrospun type II collagen tissue engineering scaffolds with carbodiimide in ethanol. Tissue Engineering 2007;13:1593-1605.

[21] Chen ZG, Wang PW, Wei B, Mo XM, Cui FZ. Electrospun collagen-chitosan nanofiber: a biomimetic extracellular matrix for endothelial cell and smooth muscle cell. Acta Biomaterialia 2010;6:372-382.

[22] Ficai A, Andronescu E, Trandafir V, Ghitulica C, Voicu G. Collagen/hydroxyapatite composite obtained by electric field orientation. Materials Letters 2010;64:541-544.

[23] Ficai A, Andronescu E, Voicu G, Ghitulica C, Vasile BS, Ficai D, et al. Self-assembled collagen/hydroxyapatite composite materials. Chemical Engineering Journal 2010;160:794-800.

[24] Gentleman E, Lay AN, Dickerson DA, Nauman EA, Livesay GA, Dee KC. Mechanical characterization of collagen fibers and scaffolds for tissue engineering. Biomaterials 2003;24:3805-3813.

[25] Huang C, Chen R, Ke QF, Morsi Y, Zhang KH, Mo XM. Electrospun collagen-chitosan-TPU nanofibrous scaffolds for tissue engineered tubular grafts. Colloids and Surfaces B-Biointerfaces 2011;82:307-315.

[26] Kirubanandan S SP. Regeneration of soft tissue using porous bovine collagen scaffold. Journal of Optoelectronics and Biomedical Materials 2010;2:141 – 149.

[27] Shen YH, Shoichet MS, Radisic M. Vascular endothelial growth factor immobilized in collagen scaffold promotes penetration and proliferation of endothelial cells. Acta Biomaterialia 2008;4:477-489.

[28] Sionkowska A, Kozlowska J. Characterization of collagen/hydroxyapatite composite sponges as a potential bone substitute. International Journal of Biological Macromolecules 2010;47:483-487.

[29] Wallace DG, Rosenblatt J. Collagen gel systems for sustained delivery and tissue engineering. Advanced Drug Delivery Reviews 2003;55:1631-1649.

[30] Wang XL, Sang L, Luo DM, Li XD. From collagen-chitosan blends to three-dimensional scaffolds The influences of chitosan on collagen nanoflbrillar structure and mechanical property. Colloids and Surfaces B-Biointerfaces 2011;82:233-240.

[31] Yusuf PS DK, Witarto AB. Application of Hydroxyapatite in Protein Purification. Makara Seri Sains 2009;13:134-140.

[32] Zhang X, Li YB, Lv GY, Zuo Y, Mu YH. Thermal and crystallization studies of nano-hydroxyapatite reinforced polyamide 66 biocomposites. Polymer Degradation and Stability 2006;91:1202-1207.

[33] Wang X NJ, Dong X, Leng H, Reyes H. Fundamental Biomechanics in Bone Tissue Engineering. In: Athanasiou Ka, editor. Morgan and Claypool Publishers, 2010:230p.

[34] Tian A, Xue XX, Liu CW, He JG, Yang ZD. Electrodeposited hydroxyapatite coatings in static magnetic field. Materials Letters 2010;64:1197-1199.

[35] Gomes PS, Santos JD, Fernandes MH. Cell-induced response by tetracyclines on human bone marrow colonized hydroxyapatite and Bonelike (R). Acta Biomaterialia 2008;4:630-637.

[36] Vallet-Regi M. Ceramics for medical applications. Journal of the Chemical Society-Dalton Transactions 2001:97-108.

[37] Theiszova M, Jantova S, Dragunova J, Grznarova P, Palou M. Comparison the cytotoxicity of hydroxyapatite measured by direct cell counting and MTT test in murine fibroblast NIH-3T3 cells. Biomedical Papers (Olomouc) 2005;149:393-396.

[38] Vani R, Girija EK, Elayaraja K, Prakash Parthiban S, Kesavamoorthy R, Narayana Kalkura S. Hydrothermal synthesis of porous triphasic hydroxyapatite/(alpha and beta) tricalcium phosphate. Journal of Materials Science: Materials in Medicine 2009;20 Suppl 1:S43-48.

[39] Braddock M, Houston P, Campbell C, Ashcroft P. Born again bone: Tissue engineering for bone repair. News in Physiological Sciences 2001;16:208-213.

[40] Eslaminejad MB, Bagheri F. Tissue Engineering Approach for Reconstructing Bone Defects Using Mesenchymal Stem Cells. Yakhteh 2009;11:263-272.

[41] Bauer TW. An overview of the histology of skeletal substitute materials. Archives of Pathology & Laboratory Medicine 2007;131:217-224.

[42] Chen J, Sotome S, Wang J, Orii H, Uemura T, Shinomiya K. Correlation of in vivo bone formation capability and in vitro differentiation of human bone marrow stromal cells. Journal of Medical and Dental Sciences 2005;52:27-34.

[43] Bronzino JD. Biomedical Engineering Handbook. In: Bronzino JD, editor. 2nd ed, CRC Press LLC, 2000:1656p.

[44] Chapekar MS. Tissue engineering: Challenges and opportunities. Journal of Biomedical Materials Research 2000;53:617-620.

[45] Sachlos E, Czernuszka JT. Making Tissue Engineering Scaffolds Work. Review on the application of solid freeform fabrication technology to the production of tissue engineering scaffolds. European Cells and Materials 2003;5:29-40.

[46] Khang G, Kim MS, Lee HB. A Manual for biomaterials/Scaffold Fabrication Technology. In: Khang G, Kim MS, Lee HB, editors. 1st ed, World Scientific Publishing Company, 2007: 288p.

[47] Eberli D. Tissue Engineering. In: Eberli D, editor. In-The 2010:524p.

[48] Prendergast PJ, McHugh PE. Topics in Bio-Mechanical Engineering. In: Prendergast PJ, McHugh PE, editors. TCBE & NCBES, 2004:252p.

[49] Liu XH, Ma PX. Polymeric scaffolds for bone tissue engineering. Annals of Biomedical Engineering 2004;32:477-486.

[50] Bolgen N, Yang Y, Korkusuz P, Guzel E, El Haj AJ, Piskin E. Three-Dimensional Ingrowth of Bone Cells Within Biodegradable Cryogel Scaffolds in Bioreactors at Different Regimes. Tissue Engineering Part A 2008;14:1743-1750.

[51] Vacanti JP. Tissue and organ engineering: can we build intestine and vital organs? Gastrointest Surg 2003;7:831–835.

[52] Langer R, Vacanti JP. Tissue Engineering. Science 1993;260:920-926.

[53] Blitterswijk CV, Thomsen P, Hubbell J, Cancedda R, Bruijn JD, Lindahl A, Sohier J, Williams DF. Tissue Engineering. In: Thomsen P, Lindahl A, Hubbel J, Williams DF, Cancedda R, Sohier J, editors. 1st ed, Academic Press, 2008, 760p.

[54] Kumar CS. Tissue, Cell and Organ Engineering. In Kumar CS, editor. 1st ed, Wiley-VCH 2007: 540p.

[55] Agrawal CM, Athanasiou KA, Heckman JD. Biodegradable PLA-PGA polymers for tissue engineering in orthopaedics. Porous Materials for Tissue Engineering 1997;250:115-128.

[56] Freed LE, Vunjaknovakovic G, Biron RJ, Eagles DB, Lesnoy DC, Barlow SK, et al. Biodegradable polymer scaffolds for tissue engineering. Bio-Technology 1994;12:689-693.

[57] Maquet V, Jerome R. Design of macroporous biodegradable polymer scaffolds for cell transplantation. Porous Materials for Tissue Engineering 1997;250:15-42.

[58] Thomson RC, Yaszemski MJ, Powers JM, Mikos AG. Fabrication of biodegradable polymer scaffolds to engineer trabecular bone. Journal of Biomaterials Science-Polymer Edition 1995;7:23-38.

[59] Simske SJ, Ayers RA, Bateman TA. Porous materials for bone engineering. Porous Materials for Tissue Engineering 1997;250:151-182.

[60] Schieker M SH, Drosse I , Seitz S, Mutschler W. Biomaterials as Scaffolds for Bone Tissue Engineering. European Journal of Trauma 2006;32:114-124.

[61] Gross KA, Rodriguez-Lorenzo LM. Biodegradable composite scaffolds with an interconnected spherical network for bone tissue engineering. Biomaterials 2004;25:4955-4962.

[62] Whang K, Healy KE, Elenz DR, Nam EK, Tsai DC, Thomas CH, et al. Engineering bone regeneration with bioabsorbable scaffolds with novel microarchitecture. Tissue Engineering 1999;5:35-51.

[63] Coombes AGA, Verderio E, Shaw B, Li X, Griffin M, Downes S. Biocomposites of non-crosslinked natural and synthetic polymers. Biomaterials 2002;23:2113-2118.

[64] Hou QP, Grijpma DW, Feijen J. Porous polymeric structures for tissue engineering prepared by a coagulation, compression moulding and salt leaching technique. Biomaterials 2003;24:1937-1947.

[65] Hutmacher DW. Scaffold design and fabrication technologies for engineering tissues - state of the art and future perspectives. Journal of Biomaterials Science-Polymer Edition 2001;12:107-124.

[66] Piskin E, Bolgen N, Egri S, Isoglu I. Electrospun matrices made of poly(alpha-hydroxy acids) for medical use. Nanomedicine 2007;2:441-457.

[67] Senkoylu A, Ural E, Kesenci K, Simsek A, Ruacan S, Fambri L, et al. Poly(D,L-lactide/epsilon-caprolactone)/hydroxyapatite composites as bone filler: An in vivo study in rats. International Journal of Artificial Organs 2002;25:1174-1179.

[68] Tuzlakoglu K, Bolgen N, Salgado AJ, Gomes ME, Piskin E, Reis RL. Nano- and micro-fiber combined scaffolds: A new architecture for bone tissue engineering. Journal of Materials Science:Materials in Medicine 2005;16:1099-1104.

[69] Basu B, Katti DS, Kumar A. Advanced biomaterials: Fundamentals, Processing and Applications. In: Basu B, Katti DS, Kumar A, editors. John Wiley& Sons, 2009:776p.

[70] Lozinsky VI. Polymeric cryogels as a new family of macroporous and supermacroporous materials for biotechnological purposes. Russian Chemical Bulletin 2008;57:1015-1032.

[71] Lozinsky VI, Galaev IY, Plieva FM, Savinal IN, Jungvid H, Mattiasson B. Polymeric cryogels as promising materials of biotechnological interest. Trends in Biotechnology 2003;21:445-451.

[72] Kathuria N, Tripathi A, Kar KK, Kumar A. Synthesis and characterization of elastic and macroporous chitosan-gelatin cryogels for tissue engineering. Acta Biomaterialia 2009;5:406-418.

[73] Dainiak MB, Allan IU, Savina IN, Cornelio L, James ES, James SL, et al. Gelatin-fibrinogen cryogel dermal matrices for wound repair: Preparation, optimisation and in vitro study. Biomaterials 2010;31:67-76.

[74] Jain E, Srivastava A, Kumar A. Macroporous interpenetrating cryogel network of poly(acrylonitrile) and gelatin for biomedical applications. Journal of Materials Science:Materials in Medicine 2009;20:173-179.

[75] Lozinsky VI, Plieva FM, Galaev IY, Mattiasson B. The potential of polymeric cryogels in bioseparation. Bioseparation 2001;10:163-188.

[76] Plieva FM, Galaev IY, Mattiasson B. Macroporous gels prepared at subzero temperatures as novel materials for chromatography of particulate-containing fluids and cell culture applications. Journal of Separation Science 2007;30:1657-1671.

[77] Ozmen MM, Dinu MV, Dragan ES, Okay O. Preparation of macroporous acrylamide-based hydrogels: Cryogelation under isothermal conditions. Journal of Macromolecular Science Part a-Pure and Applied Chemistry 2007;44:1195-1202.

[78] Hwang YS, Zhang C, Varghese S. Poly(ethylene glycol) cryogels as potential cell scaffolds: effect of polymerization conditions on cryogel microstructure and properties. Journal of Materials Chemistry 2010;20:345-351.

[79] Bloch K, Lozinsky VI, Galaev IY, Yavriyanz K, Vorobeychik M, Azarov D, et al. Functional activity of insulinoma cells (INS-1E) and pancreatic islets cultured in agarose cryogel sponges. Journal of Biomedical Materials Research 2005;75A:802-809.

[80] Bloch K, Vanichkin A, Damshkaln LG, Lozinsky VI, Vardi P. Vascularization of wide pore agarose-gelatin cryogel scaffolds implanted subcutaneously in diabetic and non-diabetic mice. Acta Biomaterialia 2010;6:1200-1205.

[81] Tripathi A, Kathuria N, Kumar A. Elastic and macroporous agarose-gelatin cryogels with isotropic and anisotropic porosity for tissue engineering. Journal of Biomedical Materials Research 2009;90A:680-694.

[82] Bhat S, Tripathi A, Kumar A. Supermacroprous chitosan-agarose-gelatin cryogels: in vitro characterization and in vivo assessment for cartilage tissue engineering. Journal of the Royal Society Interface 2011;8:540-554.

[83] Singh D, Nayak V, Kumar A. Proliferation of Myoblast Skeletal Cells on Three-Dimensional Supermacroporous Cryogels. International Journal of Biological Sciences 2010;6:371-381.

[84] Ramires PA, Cosentino F, Milella E, Torricelli P, Giavaresi G, Giardino R. In vitro response of primary rat osteoblasts to titania/hydroxyapatite coatings compared with transformed human osteoblast-like cells. Journal of Materials Science: Materials in Medicine 2002;13:797-801.

[85] Neel EA, Chrzanowski W, Knowles JC. Effect of increasing titanium dioxide content on bulk and surface properties of phosphate-based glasses. Acta Biomaterialia 2008;4:523-534.

[86] Marques AP, Gomes ME, Coutinho OP, Reis RL. Cytotoxicity screening of biodegradable polymeric systems. In: Biodegradable Systems for Tissue Engineering and Regenerative Medicine, Reis RL, Roman JS, editors. 1st edition, CRC Press, 2004: 339-353.

[87] Montanaro L, Arciola CR, Campoccia D, Cervellati M. In vitro effects on MG63 osteoblast-like cells following contact with two roughness-differing fluorohydroxyapatite-coated titanium alloys. Biomaterials 2002;23:3651-3659.

[88] Hattar S, Berdal A, Asselin A, Loty S, Greenspan DC, Sautier JM. Behaviour of moderately differentiated osteoblast-like cells cultured in contact with bioactive glasses. European Cells and Materials 2002;4:61-69.

[89] Clover J, Gowen M. Are MG-63 and HOS TE85 human osteosarcoma cell lines representative models of the osteoblastic phenotype? Bone 1994; 6: 585-591.

[90] Lanza R, Langer R, Vacanti J. Principles of Tissue Engineering. In: Lanza R, Langer R, Vacanti J, editors. 2nd ed, Academic Press, 2000: 995p.

[91] Liu E, Treiser MD, Johnson PA, Patel P, Rege A, Kohn J, Moghe P. Quantitative Biorelevant Profiling of Material Microstructure Within 3D Porous Scaffolds via Multiphoton Fluorescence Microscopy. Journal of Biomedical Materials Research 2006;79B:1-14.

[92] Bonifacino JS, Dasso M, Harford JB, Lippinxott-Schwartz J, Yamada KM. Current protocols in cell biology. In: Bonifacino JS, Dasso M, Harford JB, Lippinxott-Schwartz J, Yamada KM. Current protocols in cell biology, editors. John Wiley & Sons, 2007.

[93] Bay BH. Cytosolic calcium imaging by confocal laser scanning microscopy: applications in medicine. Singapore Medical Journal 1996;37:344-347.

[94] Stiehler M, Bunger C, Baatrup A, Lind M, Mygind T. Effect of dynamic 3-D culture on proliferation, distribution, and osteogenic differentiation of human mesenchymal stem cells. Journal of Biomedical Materials Research 2008;89A:96-107.

[95] Sabokbar A, Millett PJ, Myer B, Rushton N. A rapid, quantitative assay for measuring alkaline phosphatase activity in osteoblastic cells in vitro. Bone Miner 1994;27:57-67.

[96] Yahyouche A, Zhidao X, Czernuszka JT, Clover AJ. Macrophage-mediated degradation of crosslinked collagen scaffolds. Acta Biomaterialia 2011;7:278-286.

[97] Chang MC, Tanaka J. FT-IR study for hydroxyapatite/collagen nanocomposite cross-linked by glutaraldehyde. Biomaterials 2002;23:4811-4818.

[98] Zhai Y, Cui FZ, Wang Y. Formation of nano-hydroxyapatite on recombinant human-like collagen fibrils. Current Applied Physics 2005;5:429-432.

[99] Kim UJ, Park J, Kim HJ, Kaplan DL. Three-dimensional aqueous-derived biomaterial scaffolds from silk fibroin. Biomaterials 2005;26:2775-2785.

[100] Torres FG, Nazhat SN, Fadzullah SH, Maquet V, Boccaccini AR. Mechanical properties and bioactivity of porous PLGA/TiO2 nanoparticle-filled composites for tissue engineering scaffolds. Composites Science and Technology 2007;67:1139-1147.

[101] Santawisuk, Kanchanavasita W, Sirisinha C, Harnirattisai C. Dynamic viscoelastic properties of experimental silicone soft lining materials. Dental Materials Journal 2010;29:454-460.

[102] Wahl DA, Sachlos E, Liu C, Czernuszka JT. Controlling the processing of collagen-hydroxyapatite scaffolds for bone tissue engineering. Journal of Materials Science: Materials in Medicine 2006;18:201-209.

[103] Tao CT, Young TH. Polyetherimide membrane formation by the cononsolvent system and its biocompatibility of MG63 cell line. Journal of Membrane Science 2006; 269:66-74.

[104] Ren L, Tsuru K, Hayakawa S, Osaka A. Novel approach to fabricate porous gelatin-siloxane hybrids for bone tissue engineering. Biomaterials 2002;23:4765-4773.

[105] Bancroft J, Gamble M. Theory and practice of histological techniques. In: Bancroft J, Gamble M, editors. 6th edition, Churchill Livingstone, 2008: 725p.

[106] Sena LA, Caraballo MM, Rossi AM, Soares GA. Synthesis and characterization of biocomposites with different hydroxyapatite-collagen ratios. Journal of Materials Science: Materials in Medicine 2009;20:2395-2400.

[107] Singh R, Lee PD, Lindley TC, Dashwood RJ, Ferrie E, Imwinkelried T. Characterization of the structure and permeability of titanium foams for spinal fusion devices. Acta Biomaterialia 2009;5:477-487.

[108] Wei J, Jia JF, Wu F, Wei SC, Zhou HJ, Zhang HB, et al. Hierarchically microporous/macroporous scaffold of magnesium-calcium phosphate for bone tissue regeneration. Biomaterials 2010;31:1260-1269.

[109] Rucker M, Laschke MW, Junker D, Carvalho C, Tavassol F, Mulhaupt R, et al. Vascularization and biocompatibility of scaffolds consisting of different calcium phosphate compounds. Journal of Biomedical Materials Research 2008;86A:1002-1011.
[110] Fierz FC, Beckmann F, Huser M, Irsen SH, Leukers B, Witte F, et al. The morphology of anisotropic 3D-printed hydroxyapatite scaffolds. Biomaterials 2008;29:3799-3806.

[111] Klenke FM, Liu YL, Yuan HP, Hunziker EB, Siebenrock KA, Hofstetter W. Impact of pore size on the vascularization and osseointegration of ceramic bone substitutes in vivo. Journal of Biomedical Materials Research 2008;85A:777-786.

[112] Mu C, Liu F, Cheng Q, Li H, Wu B, Zhang G, Lin W. Collagen cryogel cross-linked by dialdehyde starch. Macromolecular Materials and Engineering 2010;295:100-107.

[113] Roveri N, Falini G, Sidoti MC, Tampieri A, Landi A, Sandri M, Parma B. Biologically inspired growth of hydroxyapatite nanocrystals inside self-assembled collagen fibers. Materials Science and Engineering C 2003;23:441-446.

[114] Chesnutt BM, Viano AM, Yuan YL, Yang YZ, Guda T, Appleford MR, Ong JL, Haggard WO, Bumgardner JD. Design and characterization of a novel chitosan/nanocrystalline calcium phosphate composite scaffold for bone regeneration. Journal of Biomedical Materials Research 2009; 88A: 491–502.

[115] Ngiam M, Liao S, Patil AJ, Cheng Z, Chan CK, Ramakrishna S. The fabrication of nano-hydroxyapatite on PLGA and PLGA/collagen nanofibrous composite scaffolds and their effects in osteoblastic behavior for bone tissue engineering. Bone 2009;45:4-16.

[116] Karageorgiou V, Kaplan D. Porosity of 3D biomaterial scaffolds and osteogenesis. Biomaterials 2005;26:5474-5491.

[117] Jayakumar R, Ramachandran R, Kumar PT, Divyarani VV, Srinivasan S, Chennazhi KP, Tamurab H, Nair SV. Fabrication of chitin–chitosan/nano ZrO2 composite scaffolds for tissue engineering applications. International Journal of Biological Macromolecules 2011;49: 274–280.

[118] Peter M, Ganesh N, Selvamurugan N, Nair SV, Furuike T, Tamura H, et al. Preparation and characterization of chitosan-gelatin/nanohydroxyapatite composite scaffolds for tissue engineering applications. Carbohydrate Polymers 2010;80:687-694.

[119] Poursamar SA, Azami M, Mozafari M. Controllable synthesis and characterization of porous polyvinyl alcohol/hydroxyapatite nanocomposite scaffolds via an in situ colloidal technique. Colloids and Surfaces B: Biointerfaces 2011;84:310-316.

[120] Bundela H, Bajpai AK. Designing of hydroxyapatite-gelatin based porous matrix as bone substitute: Correlation with biocompatibility aspects. Express Polymer Letters 2008;2:201-213.

[121] Malafaya PB, Santos TC, van Griensven M, Reis RL. Morphology, mechanical characterization and in vivo neo-vascularization of chitosan particle aggregated scaffolds architectures. Biomaterials 2008;29:3914-3926.

[122] Kelly DJ, Prendergast PJ. Prediction of the optimal mechanical properties for a scaffold used in osteochondral defect repair. Tissue Engineering 2006;12:2509-2519.

[123] Wang M. Developing bioactive composite materials for tissue replacement. Biomaterials 2003;24:2133-2151.

[124] Juhasz JA, Best SM, Bonfield W. Preparation of novel bioactive nano-calcium phosphate-hydrogel composites. Science and Technology of Advanced Materials 2010;11:1-7.

[125] Sell SA, Wolfe PS, Garg K, McCool JM, Rodriguez IA, Bowlin GL. The Use of Natural Polymers in Tissue Engineering: A Focus on Electrospun Extracellular Matrix Analogues. *Polymers* 2010; *2*:522-553.

[126] Wahl DA, Czernuszka JT. Collagen-hydroxyapatite composites for hard tissue repair. European Cells and Materials 2006;11:43-56.

[127] Song JH, Kim HE, Kim HW. Collagen-Apatite Nanocomposite Membranes for Guided Bone Regeneration. Journal of Biomedical Materials Research Part B: Applied Biomaterials 2007;83B:248–257.

[128] Moldovan L, Craciunescu O, Opríta E, Balani M, Zarnescu O. Collagen-chondroitin sulfate-hydroxyapatite porous composites: preparation, characterization and in vitro biocompatibility testing. Roumanian Biotechnological Letters 2009;14:4459-4466.

[129] Neel EA, Chrzanowski W, Knowles JC. Effect of increasing titanium dioxide content on bulk and surface properties of phosphate-based glasses. Acta Biomaterialia 2008;4:523–534.

[130] Kirkpatrick CJ, Mittermayer C. Theoretical and practical aspects of testing potential biomaterials *in vitro*. Journal of Materials Science: Materials in Medicine 1990;1:9-13.

[131] Buser D, Schenk R, Steinemann S, Fiorellini J, Fox C, Stich H. Influence of surface characteristics on bone integration of titanium implants: a histomorphometric study in miniature pigs. Journal of Biomedical Materials Research 1991;25A:889-902.

[132] Bowers KT, Keller JC, Randolph BA, Wick DG, Michaels CM. Optimization of surface micromorphology for enhanced osteoblast responses in vitro. International Journal of Oral & Maxillofacial Implants 1992;7:302-310.

[133] Martin JY, Schwartz Z, Hummert TW, Schraub DM, Simpson J, Lankford J, Dean DD, Cochran DL, Boyan BD. Effect of titanium surface roughness on proliferation, differentiation and protein synthesis of human osteoblast-like cells (MG63).Journal of Biomedical Materials Research 1995;29:389-401.

[134] Thanaphum OB, Arksornnukit M, Takahashi H, Pavasant P. Human osteoblast-like cell spreading and proliferation on Ti-6Al-7Nb surfaces of varying roughness. Journal of Oral Science 2011;53:23-30.

[135] Lincks J, Boyan BD, Blanchard CR, Lohmann CH, Liu Y, Cochran DL, Dean DD, Schwartz Z. Response of MG63 osteoblast-like cells to titanium alloy is dependeny on surface roughness and composition. Biomaterials 1988;19:2219-2232.

[136] Rosa A, Belotia MM, Van R. Osteoblastic differentiation of cultured rat bone marrow cells on hydroxyapatite with differente surface topography. Dental materials 2003;19:768-772.

[137] Tsai S-W, Hsu F-Y, Chen P-L. Beads of collagen–nanohydroxyapatite composites prepared by a biomimetic process and the effects of their surface texture on cellular behavior in MG63 osteoblast-like cells. Acta Biomaterialia 2008;4: 1332–1341

[138] Kim H-W, Kim H-E, Salih V Stimulation of osteoblast responses to biomimetic nanocomposites of gelatin-hydroxyapatite for tissue engineering scaffolds. Biomaterials 2005;26: 5221–5230.

[139] Sugimoto T, Kanatani M, Kano J, Kaji H, Tsukamoto T, yamaguchi T, Fukase M, Chihara K. Effects of high calcium concentration on the functions and interactions of osteoblastic cells and monocytes and on the formation of osteoclast-like cells. Journal of Bone and Mineral Research 1993;8:1445–1452.

[140] Dvorak MM, Riccardi D. Ca^{2+} as an extracellular signal in bone. Cell Calcium 2004;35:249–255.

[141] Dong SW, Ying DJ, Duan XJ, Xie Z, Yu ZJ, Zhu CH, Yang B, Sun JS. Bone regeneration using an acellular extracellular matrix and bone marrow mesenchymal stem cells expressing Cbfa1. Bioscience, Biotechnology and Biochemistry 2009;73:2226-2233.

[142] Liu H, Li W, Habelitz S, Gao C, Denbesten P. MEPE is downregulated as dental pulp stem cells differentiate. Archives of Oral Biology 2005; 50: 923-928.

[143] Noda M, Rodan GA. Type-β transforming growth factor inhibits proliferation and expression of alkaline phosphatase in murine osteoblast-like cells. Biochemical and Biophysical Research Communications 1986;140:56-65.